UNIVERSITE KASDI MERBAH OUARGLA
Faculté des Sciences Appliquées
Département de Génie Electrique

Mémoire
MASTER ACADEMIQUE
Domaine : Sciences et technologies
Filière : Electrotechnique
Spécialité : Machines électriques
Présenté par :

AKARTANET Aissa BENHAOUED Imad eddine

Thème:

Design Optimization Of Interior Permanent-Magnet Synchronous Motors For Wide-Speed Operation

Soutenu publiquement
Le : 15/06/2023
Devant le jury :

M^r AYAD Ahmed Nour El Islam	MCA	Président	UKM Ouargla
M^r KHALIFA Moussa	MCB	Encadreur/rapporteur	UKM Ouargla
M^me NACEUR Sonia	MCA	Examinateur	UKM Ouargla

Année universitaire 2022/2023

Dedication

With the help of ALLAH, the almighty, I was able to carry out this work

which I dedicate:

To my very dear parents in testimony of my gratitude for their patience,

their sacrifices and support throughout my studies. May ALLAH grant them

health.

To my dear sisters: Fatma ,Zahra ,Aicha ,Sakina ,Rahma and Amal.

To my dear brother :Ahmed ,Moussa ,Slimen ,Boubeker.

To all my family: Akartanet.

To all my friends who have always been there and spared no effort

to benefit me with their help and suggestions.

To all my colleagues in my class of 2022/2023.

To all those I love, without whom all of this would have no meaning….

AKARTANET Aissa

Dedication

I dedicate this modest work to:

My very dear mother,

My dear father God bless his soul,

My very dear brothers and sisters,

All my family,

And all my friends

BENHAOUED Imad eddine

Thanks

First of all we would like to thank ALLAH who helped us and gave us the patience and the courage to finish the dissertation.

We would like to warmly thank Dr. KHALIFA Moussa our Rapporteur who has made enormous efforts, through his information and his advice.

Our warmest thanks go to Mr.

president and members of the jury for accepting, reviewing and evaluating our work and all the professors in the Department of Electrical Engineering.

Our warmest thanks to all those who from near and far have contributed to the realization of this memory.

Abstract:

There are numerous electric machines utilized in industrial applications, particularly alternating current machines that function as motors or generators. Among these machines, permanent magnet synchronous machines hold significant importance due to their distinct characteristics of high torque compared to other machines. With the aid of computer technology, designing machines with permanent magnets has become possible through the utilization of the Maxwall program. Additionally, the numerical method enables us to understand the behavior of these machines. The primary objective is to digitally represent permanent magnet machines and gain knowledge about various electromagnetic phenomena, such as magnetic flux (B), magnetic field (A), and electric current, thanks to the Maxwall program.

ملخص

هناك العديد من الآلات الكهربائية في المجالات الصناعية المطبقة، ولا سيما آلات التيار المتناوب التي تعمل كمحرك أو مولد. وأهم هذه الآلات هي آلات المغناطيس الدائم المتزامنة التي تتمتع بخصائص مميزة مثل العزم الكبير والجيد، مقارنةً ببقية الآلات الأخرى. كما يمكن للحاسوب أيضًا أن يسمح لنا بتصميم آلات مع المغناطيسات الدائمة حيث يتم إجراء هذا التصميم عن طريق برنامج ماكسويل ، وبفضل الطريقة العددية، يمكن تحديد سلوك هذه الآلات. الهدف الرئيسي هو التمثيل الرقمي لآلات المغناطيس الدائم، بالإضافة إلى معرفة مختلف الظواهر الكهرومغناطيسية المتعلقة بمجال المغناطيسية (B) ومجال الكهرباء (A) والتيار الكهربائي بفضل برنامج ماكسويل.

Résumé:

Il existe de nombreuses machines électriques dans les domaines industriels appliqués, en particulier les machines à courant alternatif qui fonctionnent en tant que moteur ou générateur. Les machines synchrones à aimants permanents sont les plus importantes parmi ces machines, car elles se distinguent par leur couple élevé et leur bon fonctionnement, par rapport aux autres machines. L'ordinateur nous permet également de concevoir des machines avec des aimants permanents, ce design étant réalisé grâce au programme Maxwall. Grâce à la méthode numérique, il est possible d'identifier le comportement de ces machines. L'objectif principal est la représentation numérique des machines à aimants permanents, ainsi que la connaissance des différents phénomènes électromagnétiques tels que le flux magnétique (B), le champ magnétique (A) et le courant électrique grâce au programme Maxwall.

Summary

Summary

Summary

List of figure

List of tables

General Introduction

General introduction

In the field of electrical engineering, we have found useful industrial applications for practical life, because he developed many other sciences (mechanical, electrical, etc.), especially in the field of engine technology, because it plays an important role in the development of certain devices. Since there are several types of these machines, in particular PMSM machines, permanent magnet synchronous motors have proven to be the training system. The permanent magnet synchronous motor (PMSM) is increasingly used in industry because it offers many advantages over other types of motors direct or alternating current with high quality torque, excellent efficiency, low maintenance, low moment of inertia and high overcapacity. Synchronous motors are similar to the advent of permanent magnets (PMSM) and are increasingly used in various industrial applications such as household appliances, computers, electrical and computer equipment, and permanent magnet synchronous motors have been able to force training regimen.

1. Objective

The aim of this work is to carry out a study on the optimization of air-Gap profile in permanent magnet synchronous machines using the Maxwell program.

2. Memory structure

This thesis has been divided into three chapters :

- The first chapter consists of an overview of permanent magnet synchronous machines and equations of Maxwell of various types, in addition to mentioning the most important that help in the study of electrical machines by the computer that will be used in this study of PMSM machines
- The second chapter includes highlighting the simulation results obtained in 2 Dimensional analyzing, computing and measuring of magnetic parameters force and induced current
- The Third chapter It contains optimization about torque and air gap, how to improve them using Genetic Al-Gorithms method, and how to model and simulate magnetic field.

CHAPITRE I

Design Of PMSM In Ansys Maxwell

I.1 Introduction

In the study of any physical phenomenon, the establishment of the equations, which govern the phenomenon concerned, constitutes the first approach to the problem. All Phenomena electromagnetic signals that we generally want to study with in electrotechnical devices are governed by Maxwell's partial differential equations. The resolution of these equations associated with the laws of electrical and magnetic behavior of materials makes it possible to determine the local quantities (magnetic and electric fields, current density, etc.) and deduce global quantities (flux, current intensity, etc.). However, due to the complexity of electrotechnical systems (2D geometry, non-linearity, coupled phenomena), equations of Maxwell generally do not present an analytical solution. It is therefore necessary to have use of numerical methods by discretizing space and local quantities .

In this first chapter, we present a literature study of the different concepts, particularities related to high-speed machines, in particular permanent magnet synchronous machines(PMSM), the problem of modeling, and design of the latter as well as the methodology adopted

I.2 Permanent Magnet Synchronous Motors

Synchronous machines with permanent magnets are used more and more, during in recent years, in many fields such as automotive, aeronautics, robotics or rail transport. Due to their growing presence in increasingly diversified fields, the problems related to aging and failures of this type of actuator take a larger part in the constraints operating. The implementation of operating safety devices is well Often required in order to improve the availability of systems integrating this type of machine, to minimize the cost of maintenance and to ensure as efficiently as possible the safety of property and people directly or indirectly related to the application .[1]

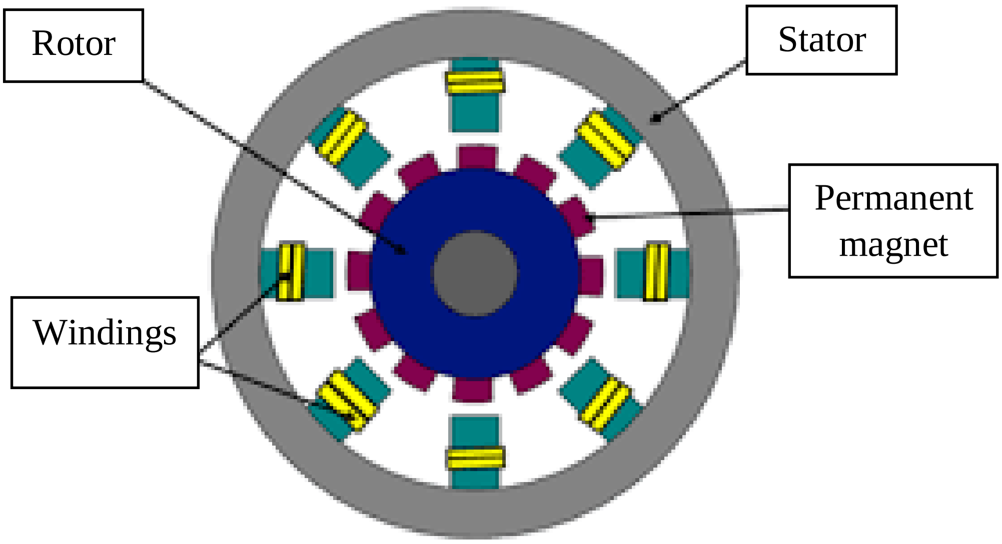

Figure.I.1 : Permanent magnet synchronous motors (PMSM)

I.3 Construction of PMSM

Wound-rotor synchronous motor like any rotating electric motor, consists of a rotor and a stator. The stator is the fixed part. The rotor is the rotating part. The stator usually has a standard three-phase winding, and the rotor is made with a field winding. The field winding is connected to slip rings to which power is supplied through brushes.

I.3.1 The Rotor

This is the rotating part. Sometimes it's a permanent magnet for small machines, but in general it is an electromagnet in the form of a massive ferromagnetic cylinder receiving a winding which, supplied with direct current (excitation), generates p pairs of south poles and alternate north. There are salient pole rotors with a high number of pole pairs p, or with smooth poles.[2]

Figure.I.2 : Rotor of PMSM

I.3.2 The Stator

The stator tooth part of the motor is composed of a plurality of teeth and grooves, and the presence of these grooves distorts the magnetic field in the air gap along the circumference.[3]

Figure.I.3 : stator of PMSM

1.4 Principles of Operation in PMSM

Currents flowing in the stator windings generate a magnetic field rotating (sliding) of the same frequency as the satirical currents. The speed of this field rotating is called synchronous speed. The magnetic poles created by magnets permanent (role of an exciter of an alternator for example) are constantly looking for align with those of the stator. This is why the machine is said to be synchronous. She can operate either in:

Generator: delivering an alternating current (production of electrical energy)

Motor: delivering a torque (production of mechanical energy)

I.5 The advantages and disadvantages of PMSM

I.5.1 The advantages

Permanent magnet synchronous machines have several advantages compared to other types of machines:

- ✓ High specific powers.
- ✓ Absence of sliding contacts.
- ✓ A good yield.
- ✓ Absence of brushes and continuous power supply.
- ✓ Ability to withstand significant transient overloads and a good dynamic behavior in acceleration and braking.[4]

I.5.2 Disadvantages

As disadvantages of the PMSM we cite:

- ✓ High cost of magnets.
- ✓ Magnetic interaction due to a change in structure.
- ✓ Influence of vibrations and shocks on the structure of the machine.
- ✓ Decrease in magnetization according to logarithmic law as a function of time.[4]

I.6 Applications of PMSM

In general, as per many researchers, we can review that the electrical motors can be applicable in many sectors like [5]

- ✓ Industrial
- ✓ Medical
- ✓ Transportation
- ✓ Automotive
- ✓ Integrated applications
- ✓ Communications
- ✓ Household appliances
- ✓ Securities

I.7 Ansys-Maxwell Software Overview

"ANSYS Maxwell" allows you not only to automate the electromagnetic calculation of electrical machines of standard design, but also to analyze the new, non-standard devices. These devices include and induction motor with ring windings.

The goals of the paper are to use "ANSYS Maxwell" for the electromagnetic calculation of induction motor with ring windings, to study program options and tools for solving such problems. A feature of the induction motor with ring windings is the fact that the magnetic system of the stator core is asymmetric and performing electromagnetic calculation can not be done in 2D, so the solution of the problem should be done in 3D. To do this, it is necessary to set design and material of the object, to determine the calculation methodology, to build a sequence of actions.

The electromagnetic characteristics of the induction motor are defined on simpler tasks for more fully understanding the principle of solving the problem within "ANSYS Maxwell". The electrical machine with the same geometric dimensions but with a classic stator and sqiurrel cage rotor is considered.[6]

I.8 Ansys Rotational Machine Expert (Rmxprt)

Rotational Machine Expert (RMxprt™) is an interactive software package used for designing and analyzing rotating electrical machines. It has some commonly used electric-machine templates. RMxprt™ can simulate and analyze the following types of machines:[11]

- ✓ Adjust-speed synchronous Machine
- ✓ Brushless Permanent Magnet DC Motors
- ✓ Claw-Pole Alternator
- ✓ Generic Rotating Machine
- ✓ Line-Start Permanent-Magnet synchronous Motor
- ✓ Permanent-Magnet DC Motor
- ✓ Single-Phase Induction Motor
- ✓ Switched Reluctance Motor
- ✓ Three-Phase Induction Motor
- ✓ Three-Phase Non Salient synchronous Machine
- ✓ Three-Phase synchronous Machine
- ✓ Universal Motor

Includes a drop-down list of tools whose main components; When ever we click on the instruction, a table will appear for us to enter the information

- ✓ The machine
- ✓ Circuit
- ✓ Stator
- ✓ Rotor
- ✓ Analysis

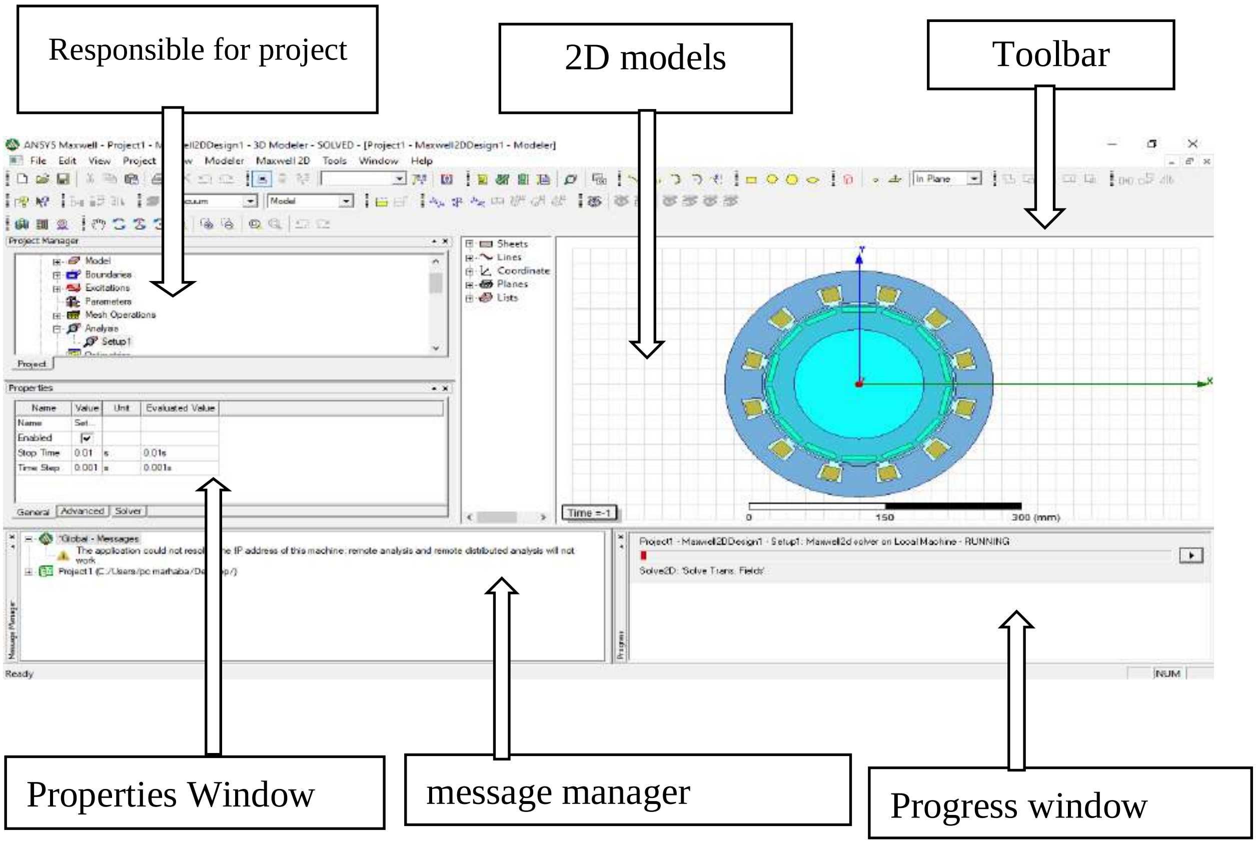

Figure.I.4 : The main window of the Maxwell software

I.9 Electromagnetic equations

I.9.1 Maxwell's equations

Maxwell's equations which govern all electromagnetic phenomena have always been the subject of in-depth research with a view to their resolution. They were established by J.C Maxwell in 1864. In the field of electrical machines, these equations have been integrated from very simplified way.

Maxwell's equations can be used in conjunction with the constitutive relations to capture the effects of particular material properties, including permeability μ conductivity σ,, and permittivity ε. In the simplest case.

Where ***E*** is the electric field intensity, **H** is the magnetic field intensity, **B** is the magnetic flux density, **J** is the current density, and **D** is the electric displacement field.

Deriving the formulation begins with Maxwell's equations, which are presented in their differential form as follows : [7]

I.9.1.1 Conservation Equations

- **Maxwell–Gauss equation**

Gauss' Law for electric fields

$$\text{Div}\,\vec{D} = \rho \tag{I.1}$$

An electric charge is the source of an electric field, in other words, the field lines

electric start and end around the electric charges.

In integral form the equation (1.1) is written in this case :

$$\int \vec{E}\,.\,\overrightarrow{dS} = \frac{q}{\varepsilon 0} \tag{I.2}$$

- **Magnetic flux conservation equation**

The corresponding formula for magnetic fields:

$$\text{Div}\,\vec{B} = 0 \tag{I.3}$$

In integral form the equation (II.3) is written in this case:

$$\int \vec{B}\,.\,ds = 0 \tag{I.4}$$

(No magnetic charge exists: no "monopoles".)

I.9.1.2 Laws of electromagnetic coupling

- **Maxwell-Faraday equations**

$$\text{Rot } \vec{E} = - \frac{\partial \vec{B}}{\partial t} \quad \text{(I.5)}$$

Thus, magnetic flux changing in time is proportional to the electromotive force. Maxwell included the Faraday's law in his Maxwell's equations, known as the Maxwell– Faraday equation.[8]

This equation expresses the electric-magnetic coupling in dynamic regime and the time variation of $\vec{D}$ determines the Rot $\vec{E}$.

The flux Φ of the magnetic field through a surface S leaning on a closed conductor is given by the relation**.** [9]

$$\Phi = \iint_S \vec{B} \text{ ds} \quad \text{(I.6)}$$

In integral form, equation (I.6) is written in this case:

$$\oint \vec{E}\, \overrightarrow{dl} = -\iint \frac{\partial \vec{B}}{\partial t} \overrightarrow{ds} \quad \text{(I.7)}$$

- **Maxwell-Ampère equation**

The Maxwell Ampere law is the start of our derivation.

$$\text{Rot } \vec{H} = \vec{j} + \frac{\partial \vec{D}}{\partial t} \quad \text{(I.8)}$$

This equation shows that the magnetic fields are produced both by the currents of conduction and by variable electric fields [∂D/∂t]; it establishes the relation ship between the fields electricity, magnetic fields and electric currents. In equation (I.8), the term ∂D/∂t is called the displacement current term In integral form the equation (I.6) is written in this case :

$$\oint_c \vec{H}\, \overrightarrow{dl} = \text{I} \quad \text{(I.9)}$$

Where **I** is the direct current inside the firm contour c. In a purely material conductor, the electrical permittivity **ε** is low. It is therefore possible to neglect the currents of displacement in equation (I.8) can thus be simplified to give Ampère's theorem.[10]

$$\text{Rot } \vec{H} = \vec{J} \quad \text{(I.10)}$$

This last equation (I.10) expresses that the circulation of the magnetic field on a contour closed on which rests a surface is equal to the sum of the currents which cross this same surface.

We deduce from equation (I.10) that the current density has a conservative flux:

$$\text{Div}\,\vec{J} = 0 \tag{I.11}$$

I.10 Machine tracing steps

Express the construction steps of an SMPM machine according to the parameters of the quadripolar machine that you are studying To keep track of the machine, fill in the following maxwell program tables:

Table I.1 : General Machine Parameters

PARAMETER	VALUE
Machine type	Adjust speed synchronous machine
Number of poles	14
Rotor position	Inner Rotor
Frictional loss	20 W
Windage loss	0 W
Reference speed	3500 rpm
Control type	DC
Circuit type	Y3

Table I.2 : General parameters of the stator

PARAMETER	VALUE
Outer Diameter	300 mm
Inner Diameter	217 mm
Length	75 mm
Stacking Factor	0.95
Steel type	Steel_1008
Number of slots	12
Slot type	4
Skew width	0

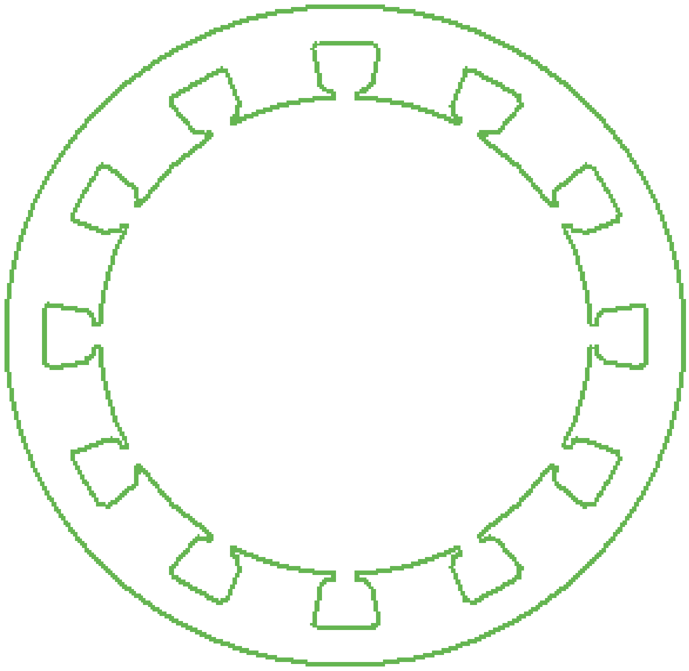

Figure.I.5 : Stator geometries

Table I.3 : General Slot Settings

PARAMETER	VALUE
Hs0	2 mm
Hs1	3 mm
Hs2	17 mm
Bs0	11 mm
Bs1	23 mm
Bs2	29 mm
Rs	2 mm

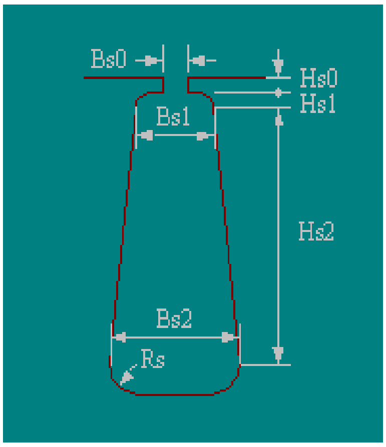

Figure.I.6 : Stator Slot Type

Table I.4 : General parameters of the winding

PARAMETER	VALUE
End Extension	7 mm
Base Inner Radius	0.3 mm
Tip Inner Diameter	1 mm
End Clearance	4 mm
Slot Liner	0.2 mm
Wedge Thickness	0.6 mm
Limited fill Factor	0.75 mm

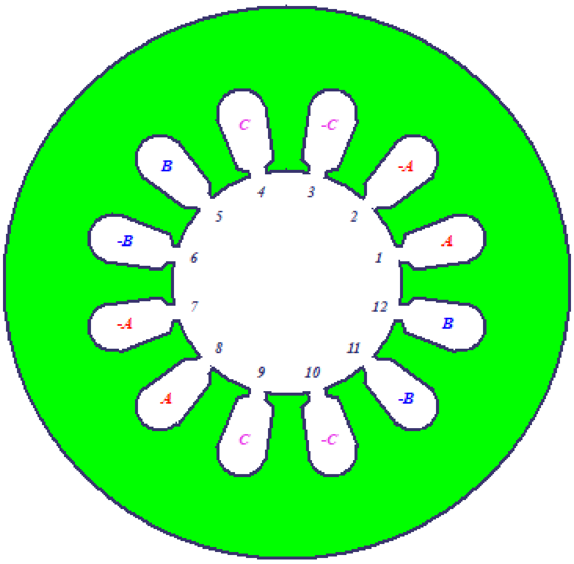

Figure.I.7 : Winding geometry

Table I.5 : General rotor parameters

PARAMETER	VALUE
Outer Diameter	210 mm
Inner Diameter	145 mm
Length	75 mm
Steel Type	Steel_1008
Stacking Factor	0.95
Pole type	5

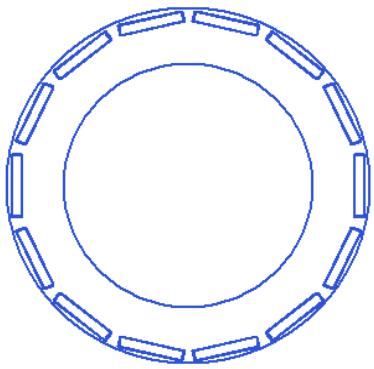

Figure.I.8 : Rotor geometries

Table I.6 : General Pole Settings

PARAMETER	VALUE
Embrace	0.8
Bridge	2 mm
Rib	0 mm
Magnet Type	NdFe30
Magnet Width	38 mm
Magnet Thick	6 mm

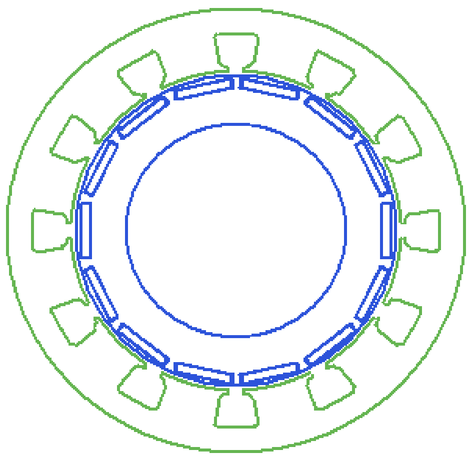

Figure.I.9 : Shaft geometry

I.11 Steps of Cumputer Aided Designe

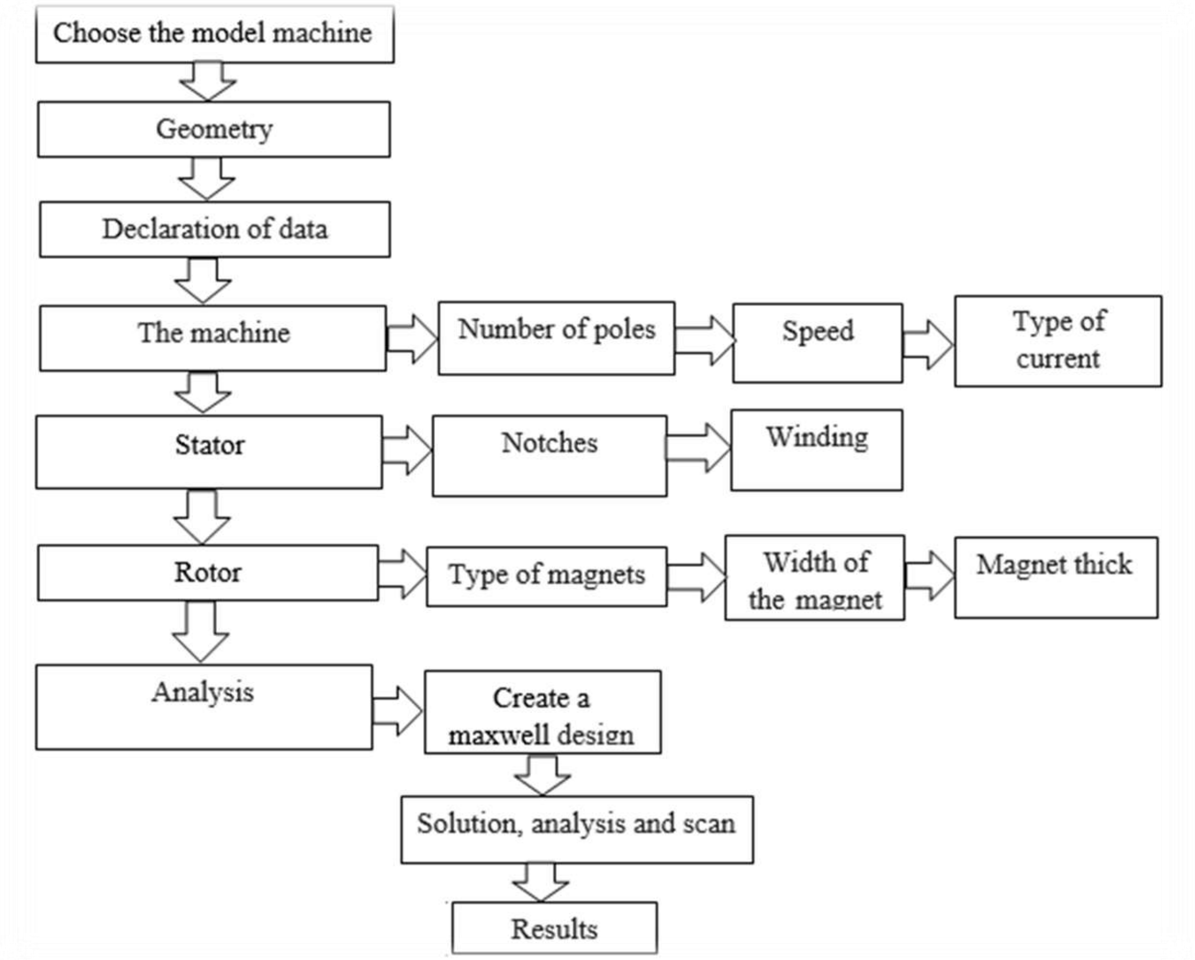

Figure.I.10 : Flowchart of the different simulation steps by Maxwell

I.12 The results

- The relation ship between input current and torque angle is shown in Figure.I.11 It can be seen from the figure that the input current of permanent magnet synchronous motor varies with the increase of the torque angle. , the input current increases rapidly to a peak of 390 A, and after reaching the peak, the acceleration begins to drop to 30 A.

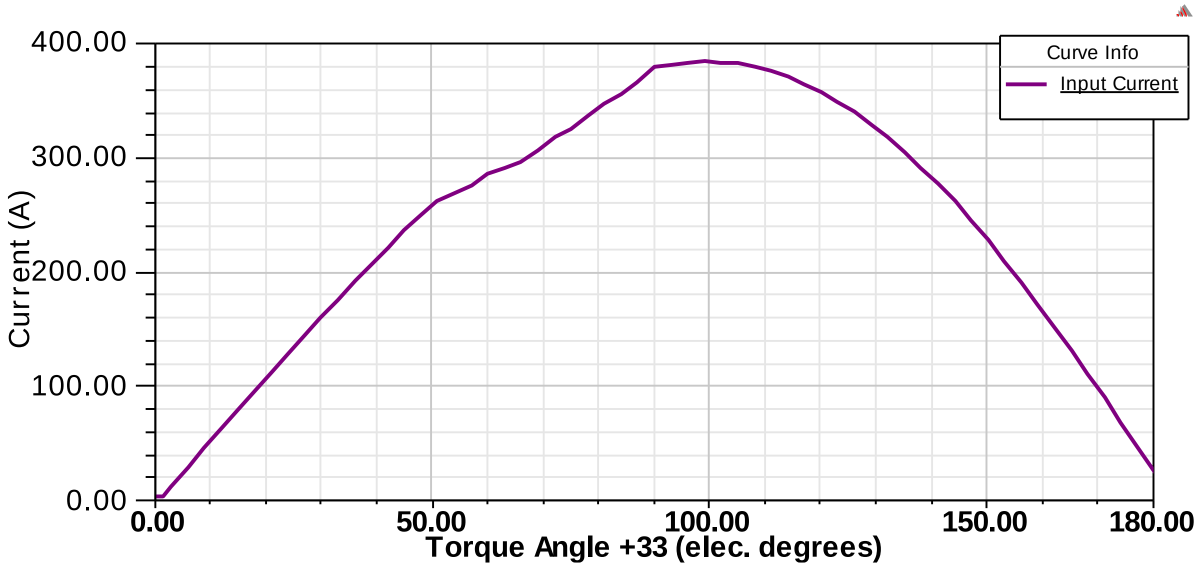

Figure.I.11 : Input Current vs Torque Angle

- The full load efficiency of PMSM was obtained after simulation of the designed model in RMxprt. The efficiency curve of the motor with respect to torque angle was found at speed through simulation. The model was simulated at 3500 rpm, and the results are shown in Figure I.12

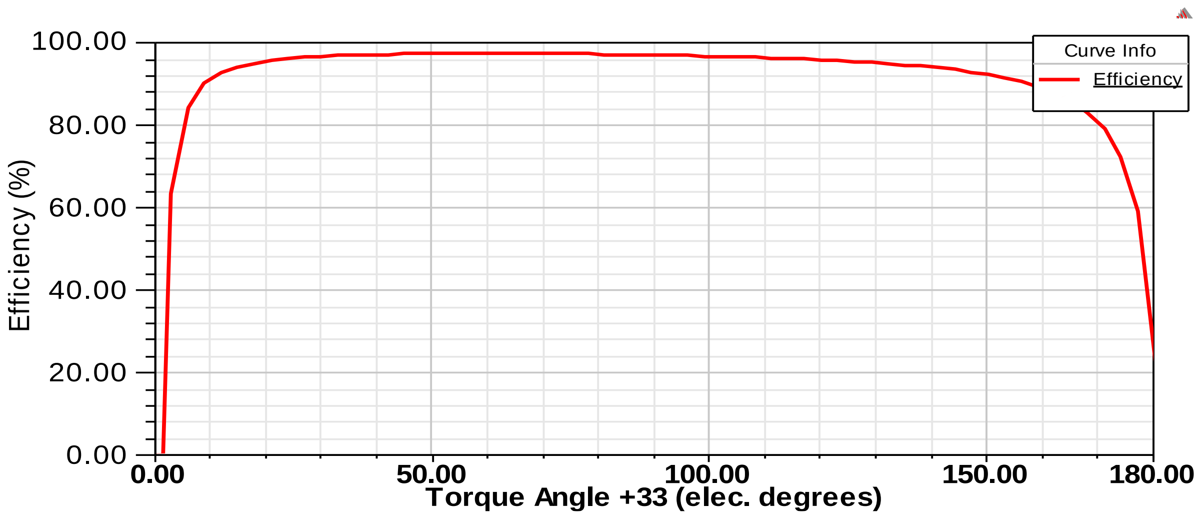

Figure.I.12 : Efficiency vs torque angle

- The torque angle vs. output power characteristics of the designed machines are obtained as shown in Figure.I.13 . The machine designed with NdFe30 has the highest output value (1.1kW) at the torque angle of approximately 100°.

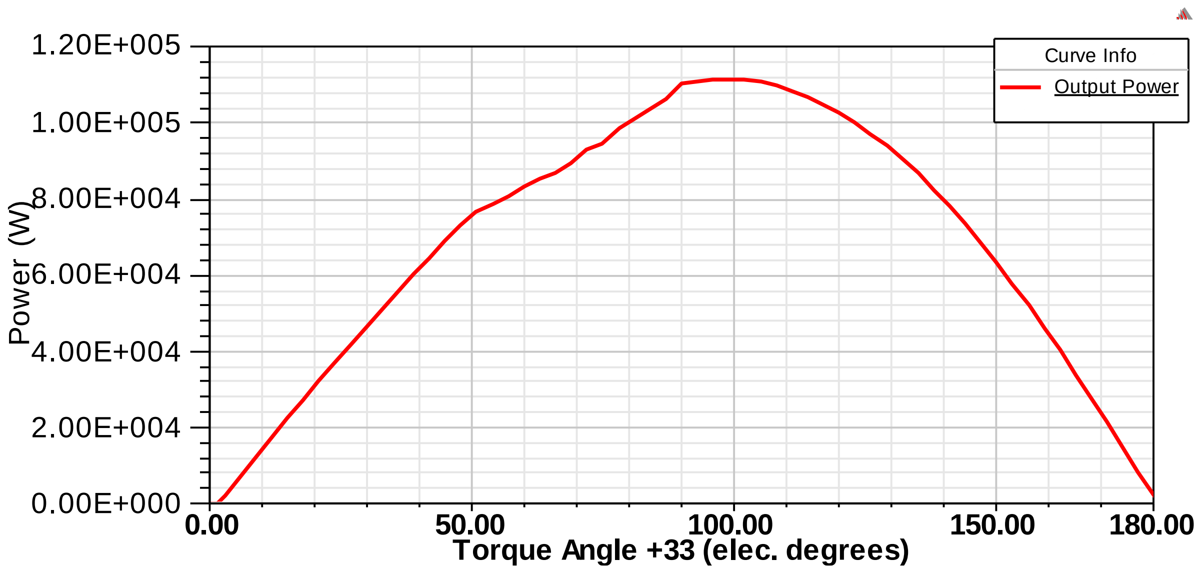

Figure.I.13 : Power Output vs Torque Angle

- Cogging torque adds harmonic content to the torque-versus-angle curves for each phase. When driven by a sinusoidal current as shown in the figure I.14.

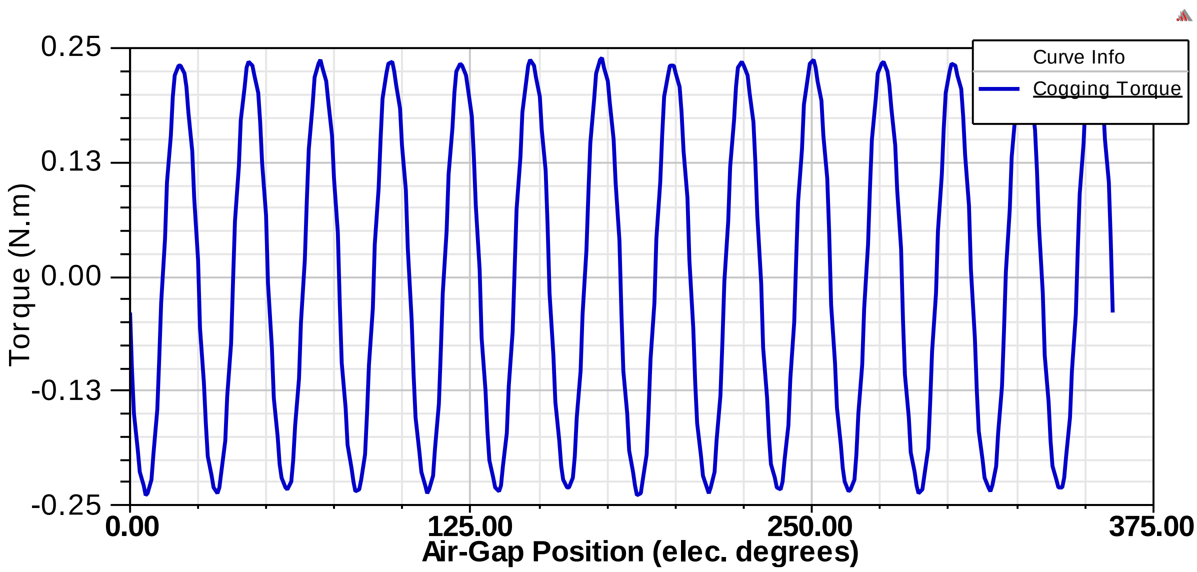

Figure.I.14 : Cogging torque in two teeth

- The relation ship between the winding voltage under load condition and electrical degree can be determined by the FEM analysis represented in Figure.I.15

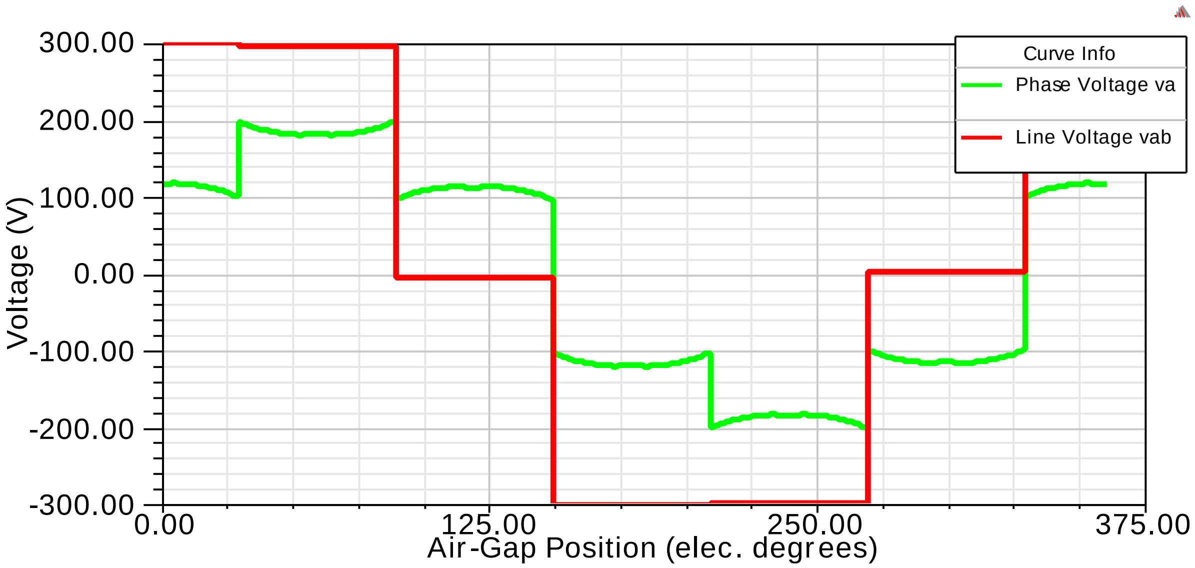

Figure.I.15 : Winding Voltages under Load

- In the figure.I.16 shows a sharp drop in the torque coefficient from 183 to 0 at torque angle 3°.

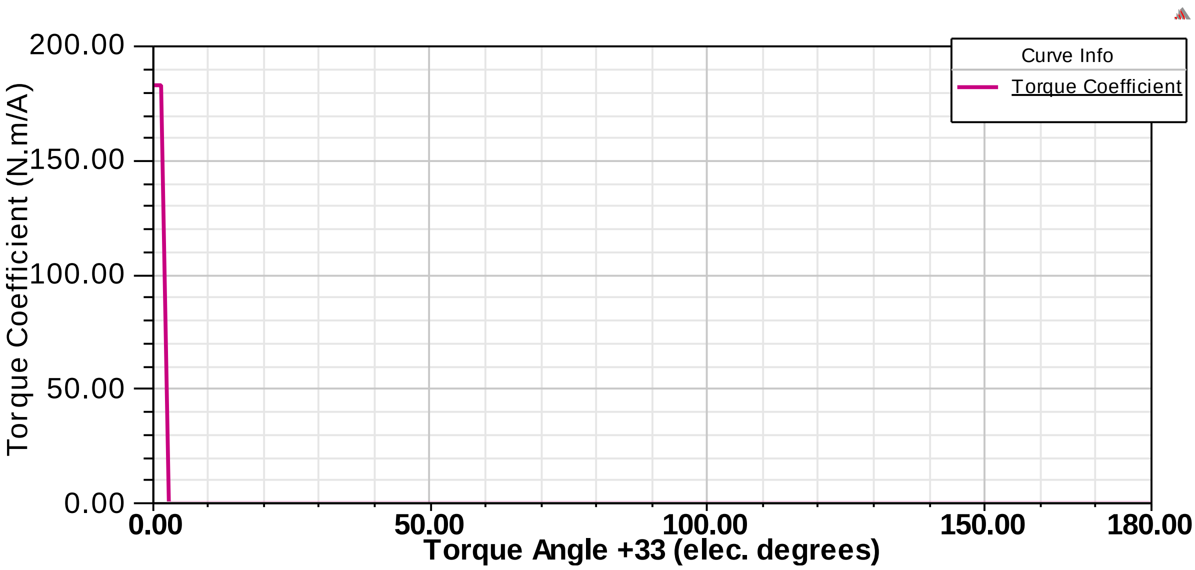

Figure.I.16 : Torque Coefficient (Torque/DC Current)vs Torque Angle

- The induced winding voltage of rated speed is shown in Figure.I.17

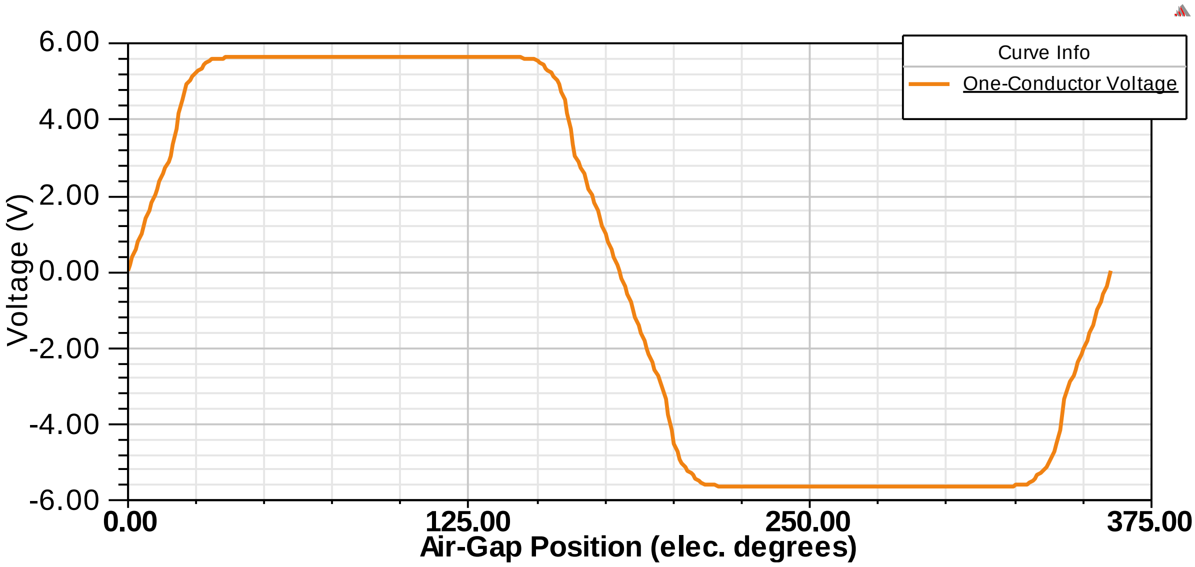

Figure.I.17 : One Conductor Indused Voltage at Rated Speed

- In this model, the maximum air-gap flux density distribution can be generated about 0.5 T by Maxwell 2D.The important parameter of air-gap flux density distribution of PMSG as shown in Figure.I.18.

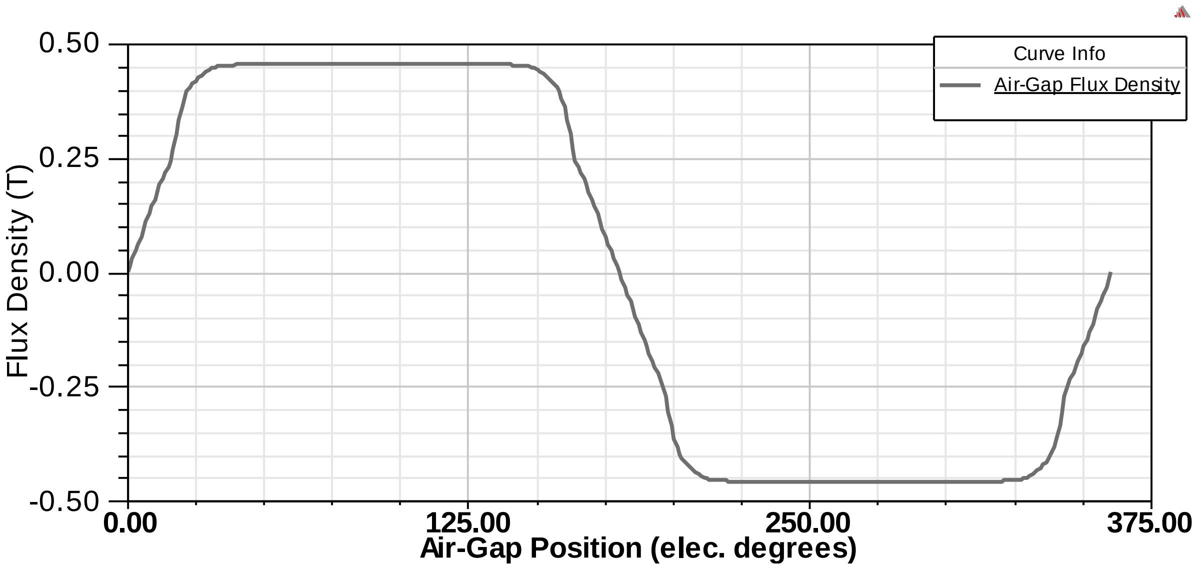

Figure.I.18 : Air-Gap Flux Density

I.12. Conclusion

In this chapter, we were able to familiarize ourselves with Maxwell 16.0. in the first place we used the RMxprt software application to determine the architecture of our devices by the performances of the PMSM machine were determined by simulation in order to study a specific performance of a machine in a dynamic system (Transient) We have created a 2D model from RM xprt where we simulated the machine the results obtained show the effectiveness of Maxwell 2D software to identify and analyze the speed and torque of machines synchronous to permanent magnet.

CHAPITRE II

Electromagnetic Analysis of PMSM

II.1 Introduction

Maxwell is a 64-bit Windows program that can process geophysical data at from electromagnetic and electromagnetic surveys. It is used by professionals the mining industry, consultants and academics around the world. It is the tool of processing and interpretation par excellence for those who process geophysical data electromagnetic and electrical. Developed and maintained by professionals.

In this chapter, we study the theoretical study of PMSM machines using this logistics with RMxprt and 2D functionalities, this study aims to represent the method digital FEM of the PMSM machines and to show all the phenomena and their behavior theoretically by computer.

II.2 Maxwell 2D

Maxwell 2D is a high-performance, low frequency electromagnetic field simulation interactive software package that uses finite element analysis (FEA) to solve electromagnetic problems by solving Maxwell's equations in a finite region of space with appropriate boundary and user-specified initial conditions for 2D/3D electromagnetic and electromechanical devices, including motors, actuators, transformers, sensors and coils. Maxwell uses the accurate finite element method to solve static, frequency-domain, and time-varying electromagnetic and electric fields. The software can only use a triangular/tetrahedral elements to mesh the domain and linear interpolation functions to approximate the solution [12]

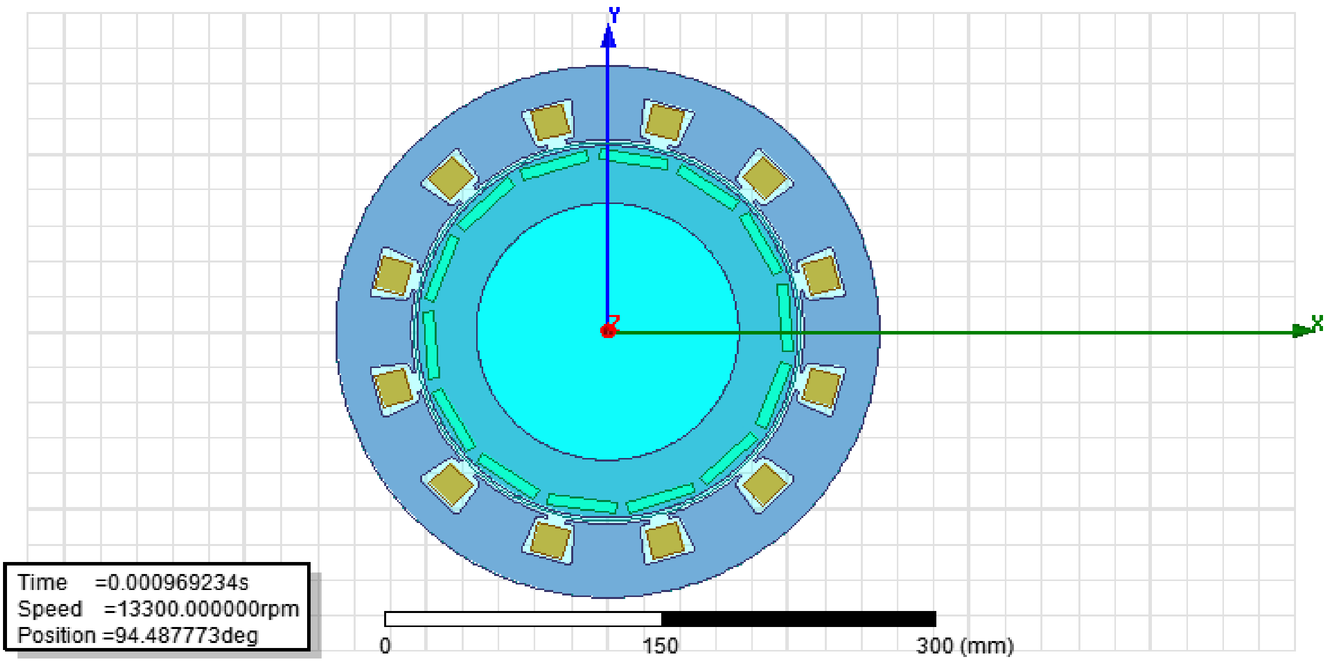

Figure.II.1 : 2D machine geometry

II.3 Finite Element Method

There are number of technic which have been developed to solve electromagnetic related problems not amenable to exact solution. The Finite element method is used to convert the complex partial differential equation into nonlinear algebric equation The finite element method can be applied to the vector Helmholtz wave equation, which is derived from the Maxwell's equations, or it can be derived from a scalar-vector potential formulation of the fields. There are variety of commercial geometrical modelling tools to accurately model any three–dimensional geometry and to generate the required mesh with any kind of elements such as triangles, tetragonals and hexagonals[13].

FEM involves the following for the solving a boundary value problem:

- ❖ Discretization of the domain
- ❖ Derivation of the element equations
- ❖ Assembly of the elements
- ❖ Solutions of the system equations

II.4 Principle of the finite element method

The principle of the FEM lies in the division of the elementary domain of finite dimensions on each domain called finite element, the unknown function is approached by a tooth polynomial the degree can vary from one application to another[14].

The main stages of construction of a finite element method are the following:

- ✓ Discretization of the continuous environment, representing the field of study in sub-field (element).
- ✓ Construction of the nodal approximation by subdomain.
- ✓ Calculates elementary matrices (for each element) corresponding to the integral from of the problem.
- ✓ Assembly of elementary matrices taking into account the boundary conditions.
- ✓ Solving the equation system.

There are different types of elements:

- linear element (1D).
- Surface element (2D).
- Volume element (3D) [2].

In our case, the field of study, which is two-dimensional, we often meet with linear, quadratic or cubic elements. To lead to a better accuracy of the solution, one proceeds to refine the mesh see Figure.II.2.

- ❖ One-dimensional problem (straight element)

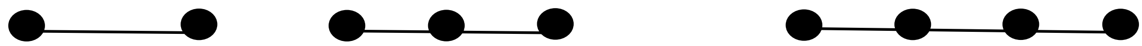

Linear (02 nodes) quadratic (03 nodes) cubic (04 nodes)

- ❖ Two-dimensional problem (triangle or quadrilateral)

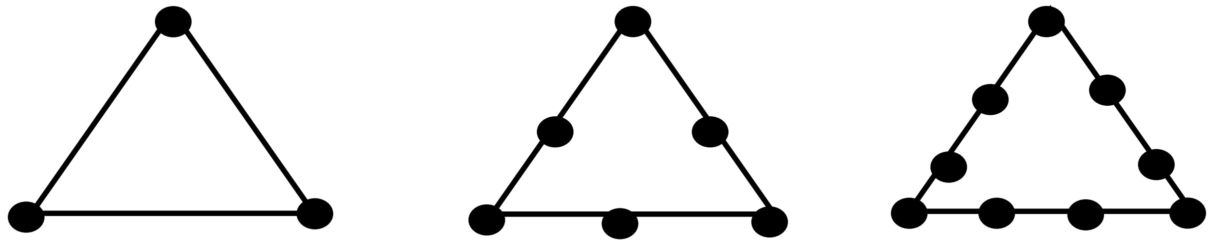

a) Linear element (03 nodes) b) quadratic (06 nodes) c) cubic (09 nodes)

- ❖ Three-dimensional problem

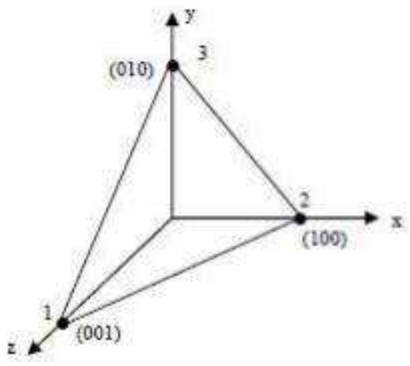

Linear element (04 nodes)

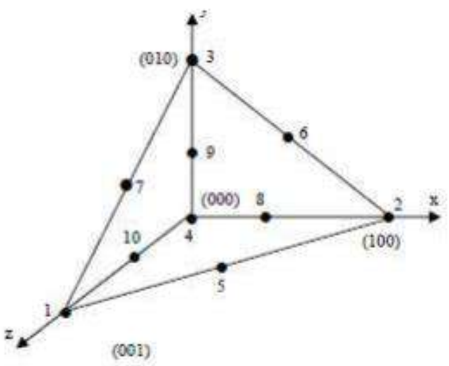

Quadratic element (10 Nodes)

Figure.II.2 : Discretization of the study domain (mesh) [15]

II.5 Finite Modeling of Permanent Magnets

The hysteresis characteristic equation for the permanent magnet can be inserted into amperes law (without displacement currents) and then discretized. This is done to get equation II.1[16]

$$\nabla \times [\upsilon \mathrm{B} - \mathrm{Hc}] = \mathrm{J}_{\mathrm{ext}} \quad \text{(II.1)}$$

The coercive force of the permanent magnet (excitation) in equation II.34can be moved over to the right side of the get equation II.2

$$\nabla \times (\upsilon \mathrm{B}) = \mathrm{J}_{ext} + \nabla \times H_{\mathrm{c}} \quad \text{(II.2)}$$

The equation can also be solved with respect to the magnetization vector [16], as in equation II.3

$$\nabla \times (\upsilon \mathrm{B}) = \mathrm{J}ext + \nabla \times (\upsilon \mu_0 \mathrm{M}) \quad \text{(II.3)}$$

In the same way, it is possible to solve the equation with respect to the magnetic vector potential.

$$\nabla \times (\upsilon \nabla \times \mathrm{A}) = \mathrm{J}_{ext} + \nabla \times \mathrm{Hc} \quad \text{(II.4)}$$

In 2D analysis, there is no excitation from the permanent magnet in the z-direction. The curl of the excitation can then be simplified in two dimensions.

$$\frac{\partial}{\partial \mathrm{x}} [\upsilon \frac{\partial \mathrm{Az}}{\partial \mathrm{x}}] + \frac{\partial}{\partial \mathrm{y}} [\frac{\partial \mathrm{Az}}{\partial \mathrm{y}}] = -\mathrm{J}_{ext} + \frac{\partial \mathrm{Hcx}}{\partial \mathrm{y}} - \frac{\partial \mathrm{Hcy}}{\partial \mathrm{x}} \quad \text{(II.5)}$$

The only region where there is a coercive force is in the permanent magnet region, but the sources of diffusion applies only at the boundaries of the PM where Hc changes to zero. It is easy to see that the permanent magnet has a current winding equivalent (HI=NI)

II.6 Cumputer Aided Designe phases

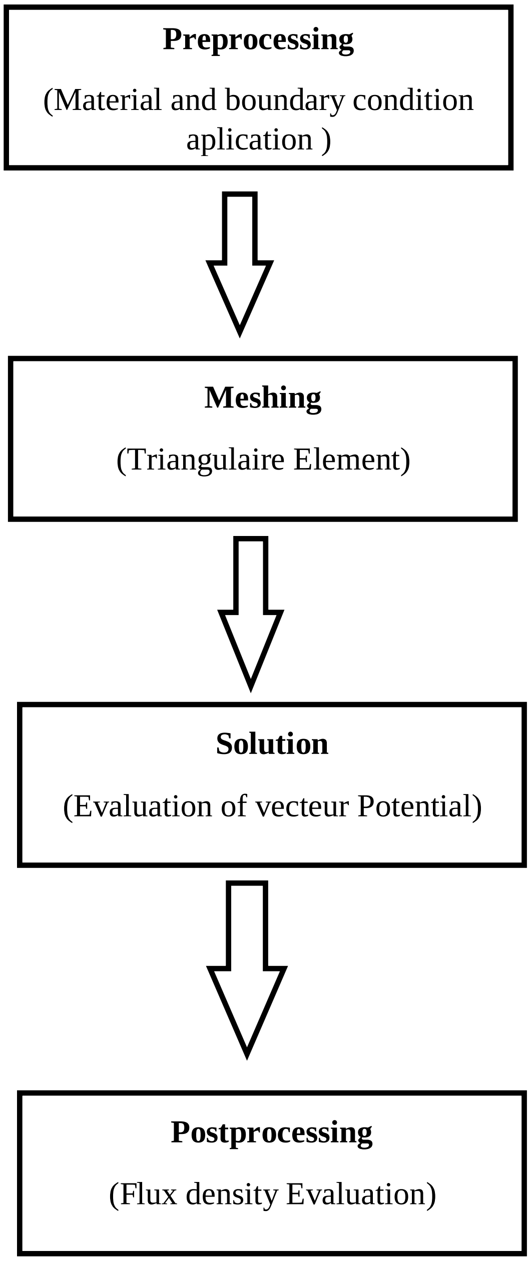

Figure.II.3 : Flowchart of finite element method

II.7 Cogging Torque Minimisation

he torque ripple in PMSM is primarily caused by the cogging torque developed between the stator teeth and rotor permanent magnet poles. Gap energy variation can be used to calculate the cogging torque developed [17].

$$M_{cog}(\theta) = -\frac{dE(\theta)}{d\theta} \quad \text{(II.6)}$$

$$E(\theta) = -\frac{1}{2\mu}\int BdV \quad \text{(II.7)}$$

where E represents the net energy of air-gap between the rotor and stator relative to the space angle θ The spatial energy distribution in the machine airgap is given in Equation

$$M_{cog} = -\frac{Lnet\Delta^2 g\alpha gap}{\mu 0(\alpha\pi)^2}\sum_{n=1}^{\infty}\frac{1}{n}\sin\left(n\frac{Ns}{g}\theta\right) \quad \text{(II.8)}$$

$$\mathrm{Sin}\left(n\frac{Ns\,Np\,SI0}{2g}\right)\sin\left(n\frac{Ns\,Np}{2g}\,\theta - n\frac{Ns\,Np\,SIp}{2g}\right)$$

where B corresponds to the flux density distribution in various parts of the PMSM including the air-gap. In the iron part, the energy variation is negligible because of the negligible reluctance of the iron path. The air-gap flux density distribution can be calculated from the product of airgap flux density distribution of a slotless machine and the relative permeance function of the air-gap.[18]

$$B = P(\beta,z)B(\beta,\theta) \quad \text{(II.9)}$$

where P(β,z) is the relative permeance of air-gap and P(β,z) is the equivalent airgap flux density of a slotless machine. From Equation (11), the energy distribution of Equation (10) can be determined as follows:

$$E(\theta) = -\frac{1}{4\mu 0}(r_2^2 - r_1^2)\int_0^{Lnet}\int_0^{2x} P^2 gab(\beta,z)B^2(\beta,\theta)d\beta dz\ L_{net} \quad \text{(II.10)}$$

where μ_0 is the permeability of free space; r_2 and r_1 are the outer and inner radii of the air-gap, respectively. β is the circumferential angle, L_{net} is the machine bore length, and z is the position along the machine axis.

II.8 The results

- The figure below represents the torque as a function of time:

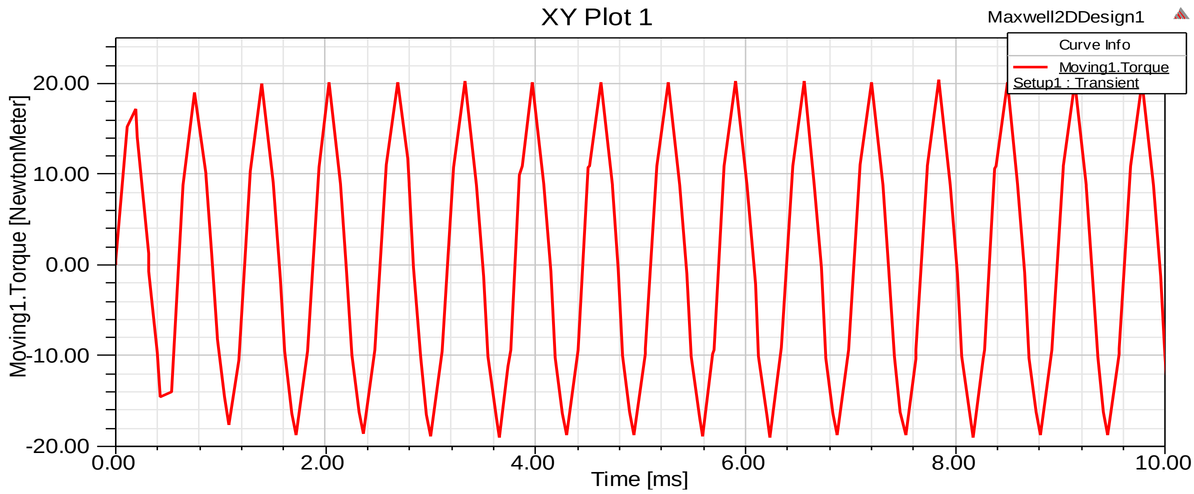

Figure.II.4 : The torque curve

- The figure below represents winding current as a function of time:

windings of phases b and c are identical to a and are displaced from it by 120◦ and 240◦ , respectively

$ia = Im \cos(\omega t)$

$ib = Im \cos(\omega t - 120^{\circ})$

$ic = Im \cos(\omega t + 120^{\circ})$

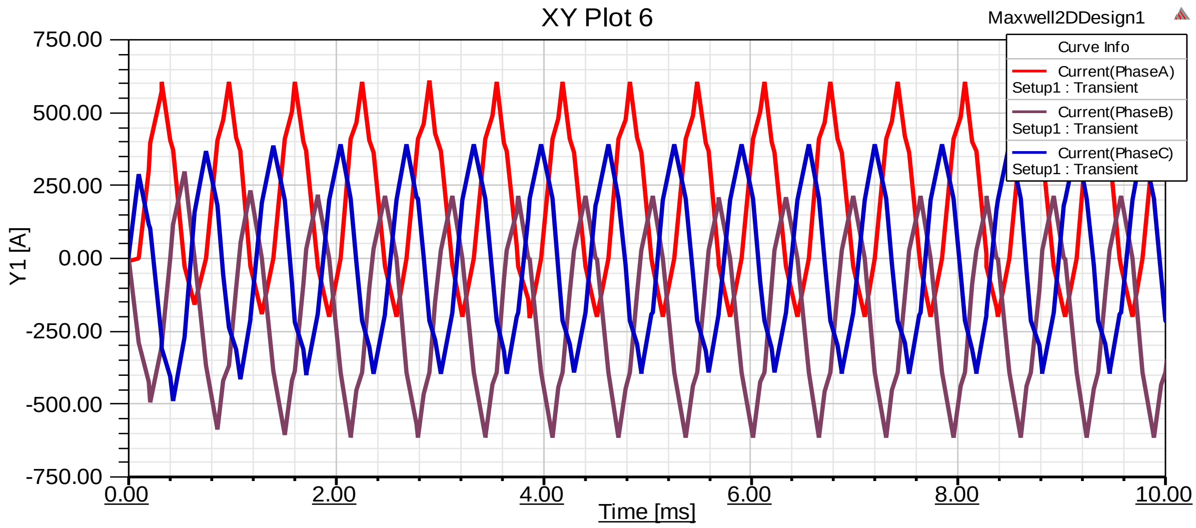

Figure.II.5 : Induced Winding Voltages of Phase A, B, and C

➢ **Air Gap**

- The figure below represents the magnetic induction as a function of the distance :

Figure.II.6 : The magnetic induction curve of Air Gap

- The figure below represents the magnetic field as a function of the distance :

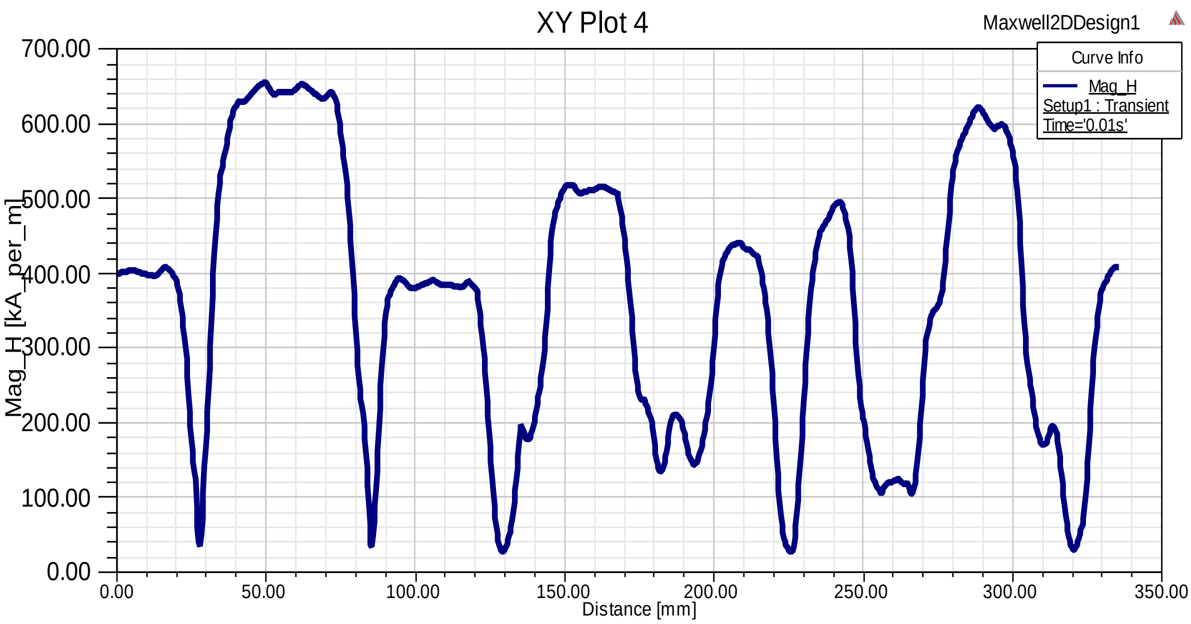

Figure.II.7 : The magnetic field curve of Air Gap

- The figure below represents the energy as a function of the distance :

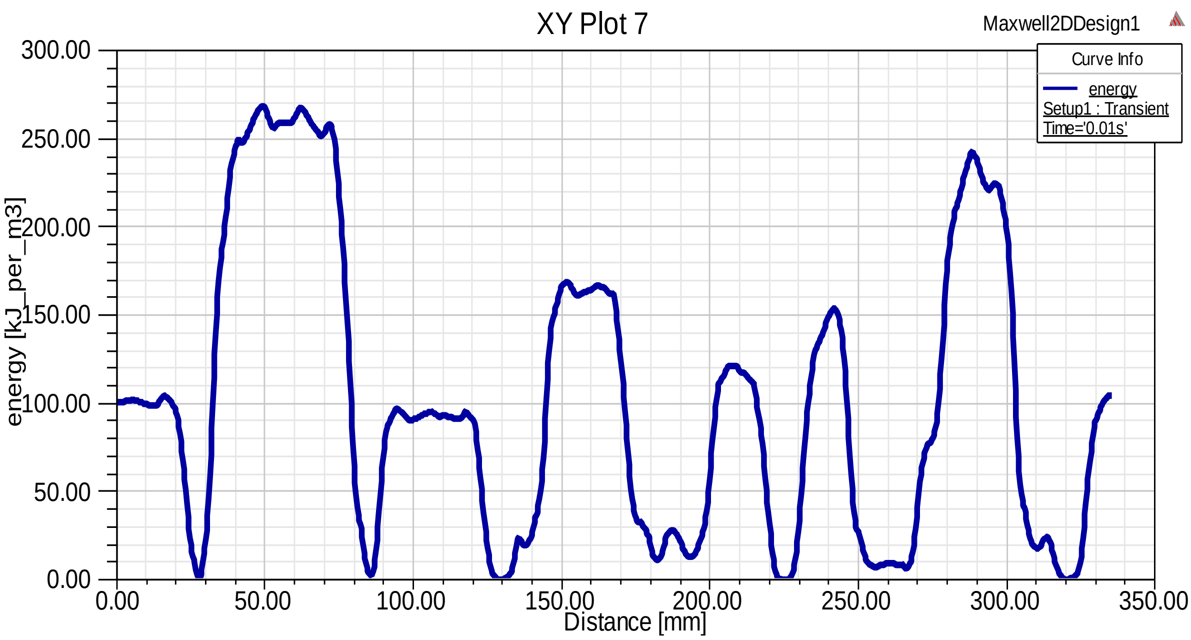

Figure.II.8 : Energy curve of Air Gap

➢ **Stator**

- The figure below represents the magnetic induction as a function of the distance :

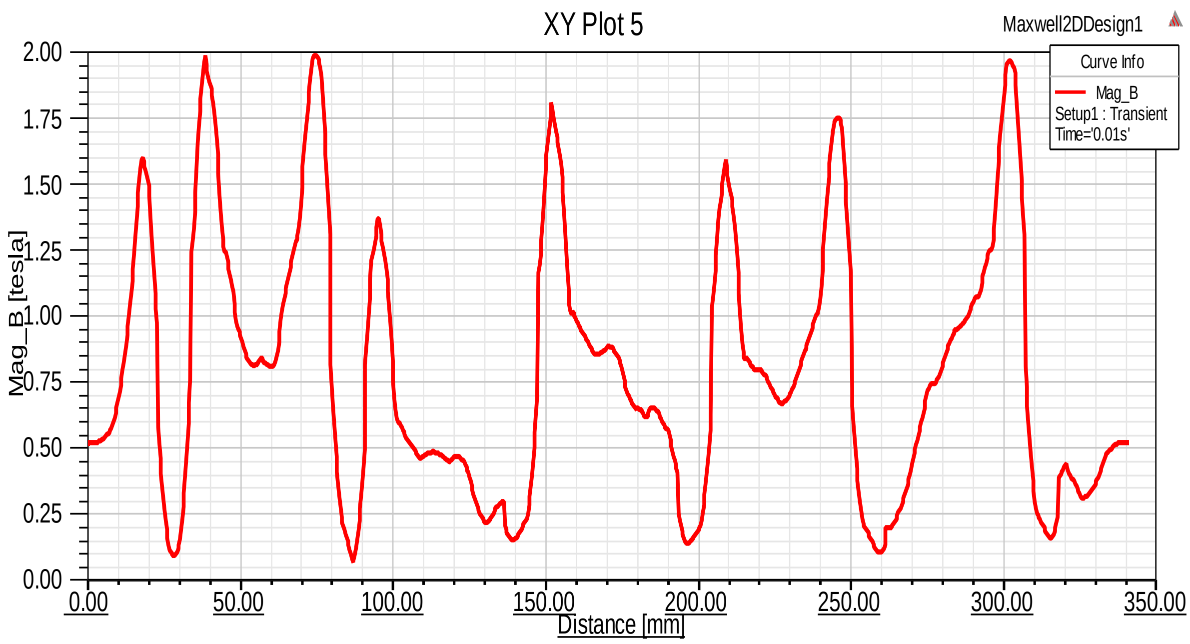

Figure.II.9 : The magnetic induction curve of the Stator

- The figure below represents the magnetic field as a function of the distance :

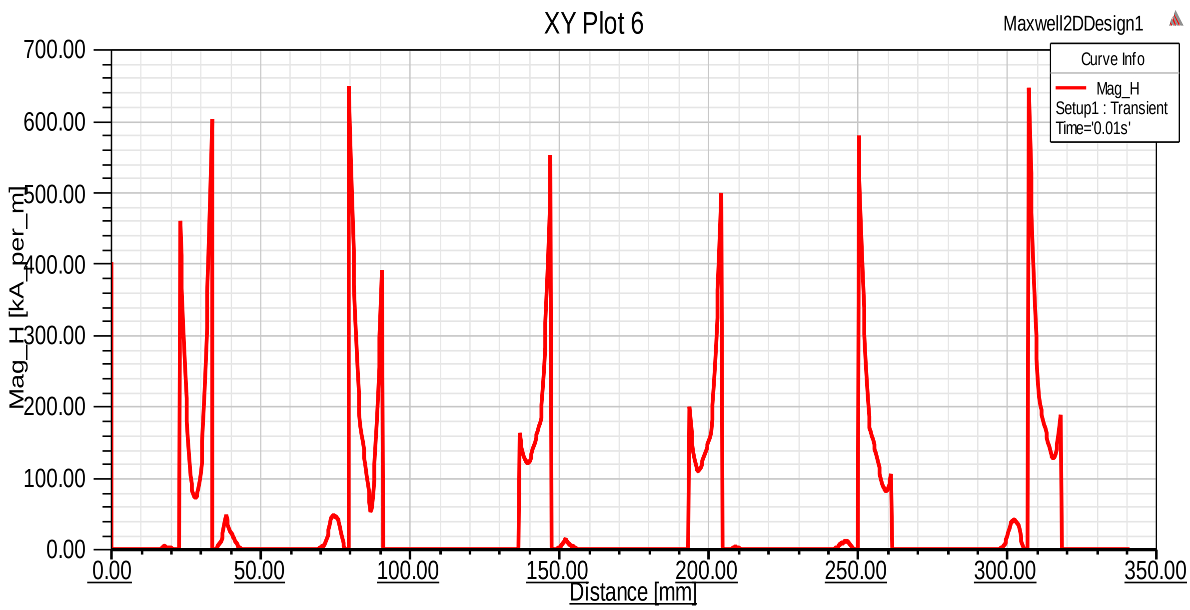

Figure.II.10 : The magnetic field curve of the Stator

- The figure below represents the energy as a function of the distance :

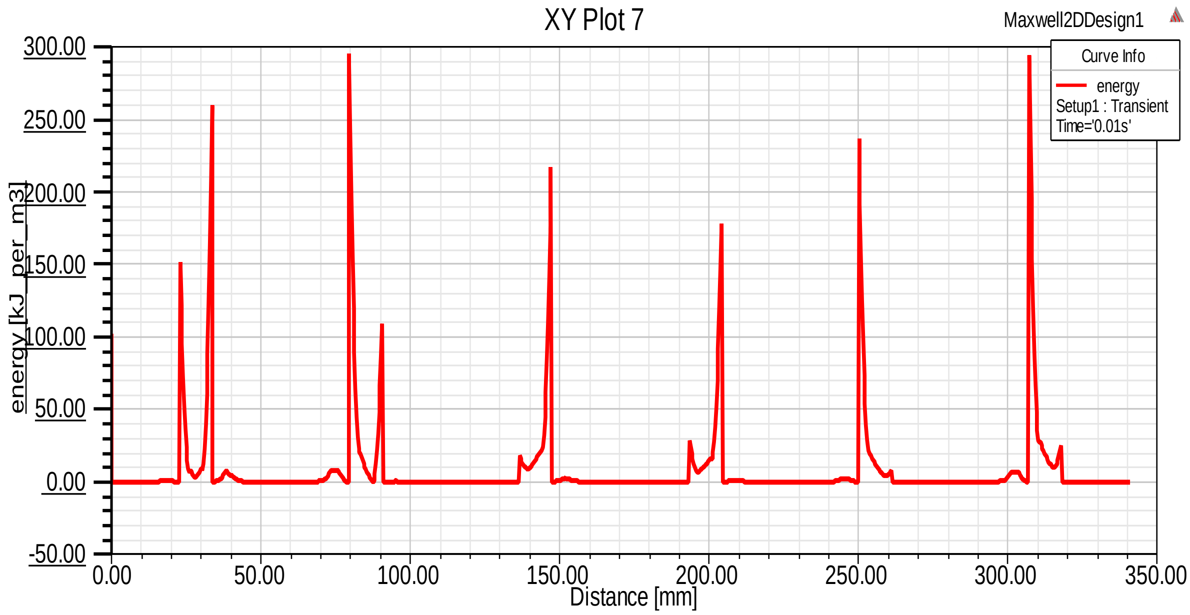

Figure.II.11 : Energy curve of the Stator

➢ **Rotor**

- The figure below represents the magnetic induction as a function of the distance :

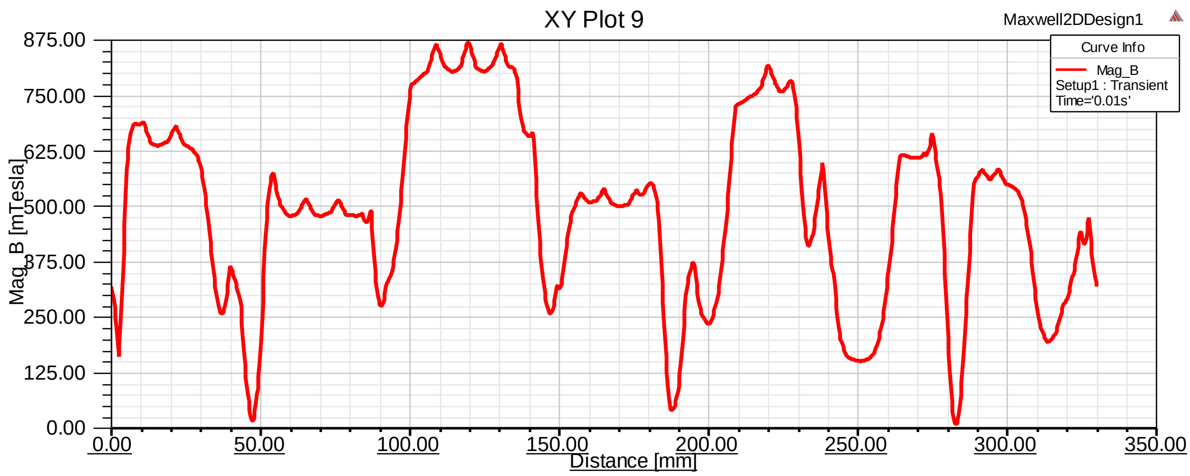

Figure.II.12 : The magnetic induction curve of the Rotor

- The figure below represents the magnetic field as a function of the distance :

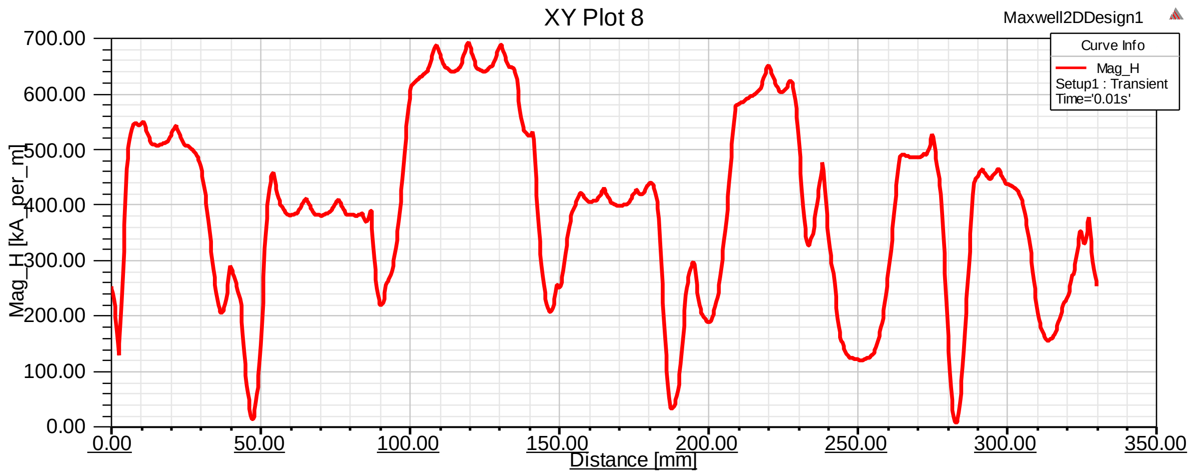

Figure.II.13 : The magnetic field curve of the Rotor

- The figure below represents the energy as a function of the distance :

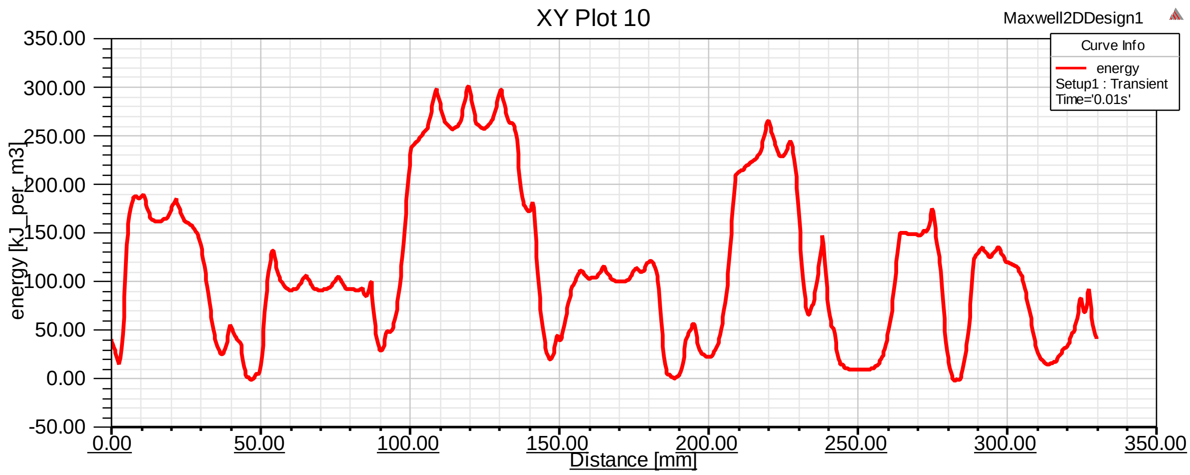

Figure.II.14 : Energy curve of the Stator

II.9 Conclusion

In this chapter, we were able to familiarize ourselves with Maxwell 16.0
Before that, we used RMxprt software in the first chapter to determine the structure of the machine, then the performance of the synchronous magnet machine permanent were determined by simulation in order to study the specific performances of the machine in a dynamic system. the effectiveness of the Maxwell 2D program for determine and analyze the performance of permanent magnet synchronous machines.

CHAPITRE III

Optimization Of PMSM Based GA Method

III.1 Introduction

In this chapter we study and implement the optimisation of PMSM used genetic al-gorithms (GA) method in maxwell software and RMxprt based on the previous model of chapter II. he numerical modeling and simulation with maxwell software based on GA method to solve equations and many problems The desing result help to show the optimisations and around of the magnetic field in motor and dynamic state (rotate).

III.2 Genetic Al-Gorithms (GA) Method

GA method is applied in the minimization of the cogging torque by optimizing the three motor parameters: the magnet thickness, the magnet shape and the pole embrace the coverage of the rotor with the magnets or the magnet span. Firstly, a motor model suitable for computer-aided design is modeled and its ac-curacy is verified by comparing the output results of this model with the available data from the motor producer.

Afterwards, the GA method is applied on the existing computer model, which yielded to the best set of data for the magnet thickness; the pole shape and the pole embrace that produce the minimal cogging torque. The GA had searched the complete space of the possible solutions and had found the best combination of these three parameters that yielded to the global minimum of the optimization function in this case the cogging torque. There sults from the GA optimization regarding these three parameters were applied in the optimized model and there maining operating characteristics were obtaine [19].

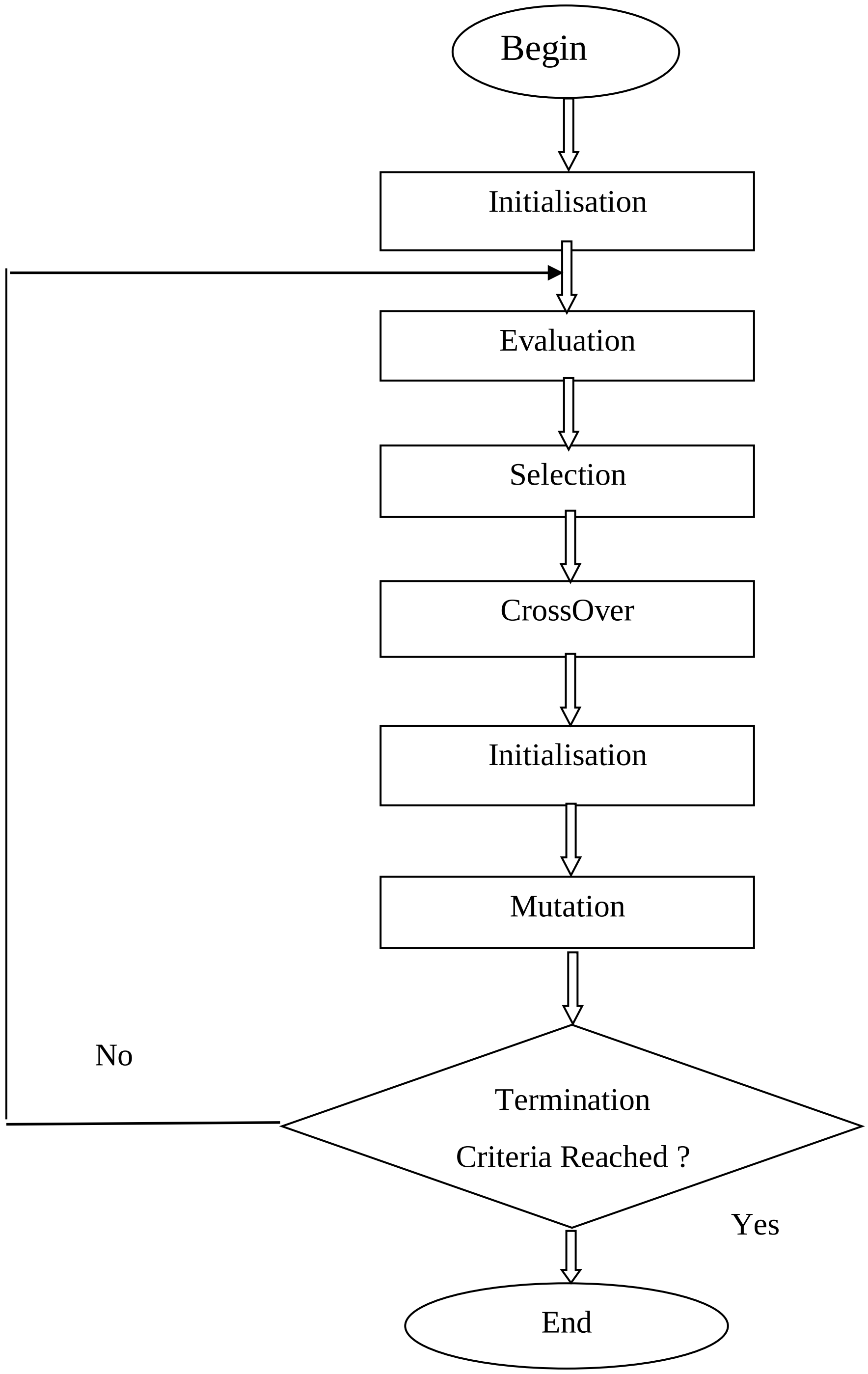

Figure.III.1 : Genetique Algorithm FlowChart [21]

III.3 Optimization used Maxwell softwer

The Ansys Maxwell electromagnetic software has been employed to analyse the distribution of the magnetic flux density in the magnetic cores o the excited sensors. To simplify the design diversity despite the distinct geometric designs of the excitation coils, key design factors were maintained unchanged through the various designs to allow for comparisons. This includes the number of wires turns, the metal wire gap, the cross-sectional area of the metal wire, the coil resistance, the coil inductance and the dimensions of the ferromagnetic core[20].

The optimization model of the motor was created using GA method with random search Setting of the model was based on the recommendation from the soft-ware producer, and the time required the optimization problem to be solved. Cost function is optimized with respect to three calculation setups: cogging torque, average value of magnetic flux density in the air gap and magnet area

III.4 Optimal Pole Embrace

In this study, Ansys RMxprt and Maxwell modules are used for initial machine design 2D analyses are done according to best performance results. Most attention is given to pole embrace parameter for minimum cogging torque. Pole embrace is the ratio of magnetic pole as shown in Figure.1. The values used in this study are calculated according to this formula. After various optimizations, the parameters which gave minimum cogging torque are obtained[22]

Dimensions related to magnet poles are presented in Figure.2.

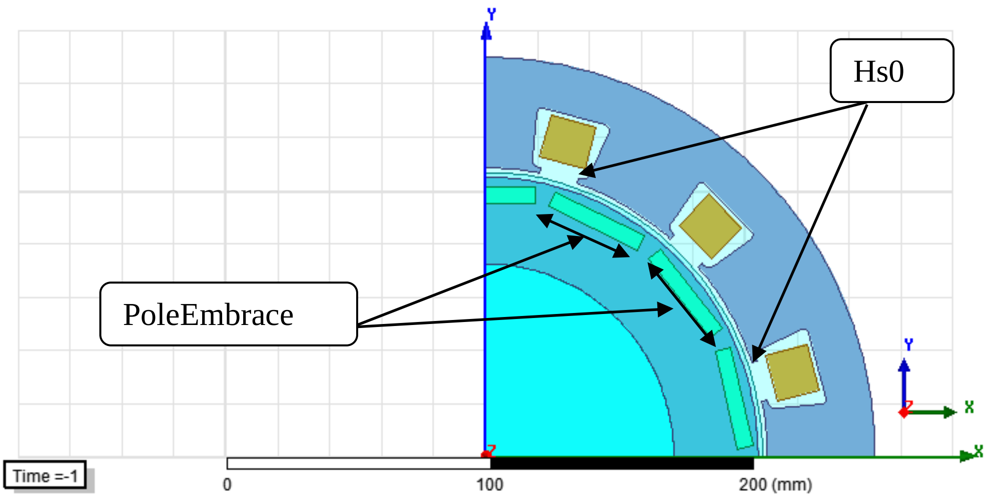

Figure.III.2 : Geometry of analyzed parameters.

III.5 The results

- After the optimization is done, the results are available in a graphic form thus the variation of the cost function through the iterations is presented in Figure.III.3.

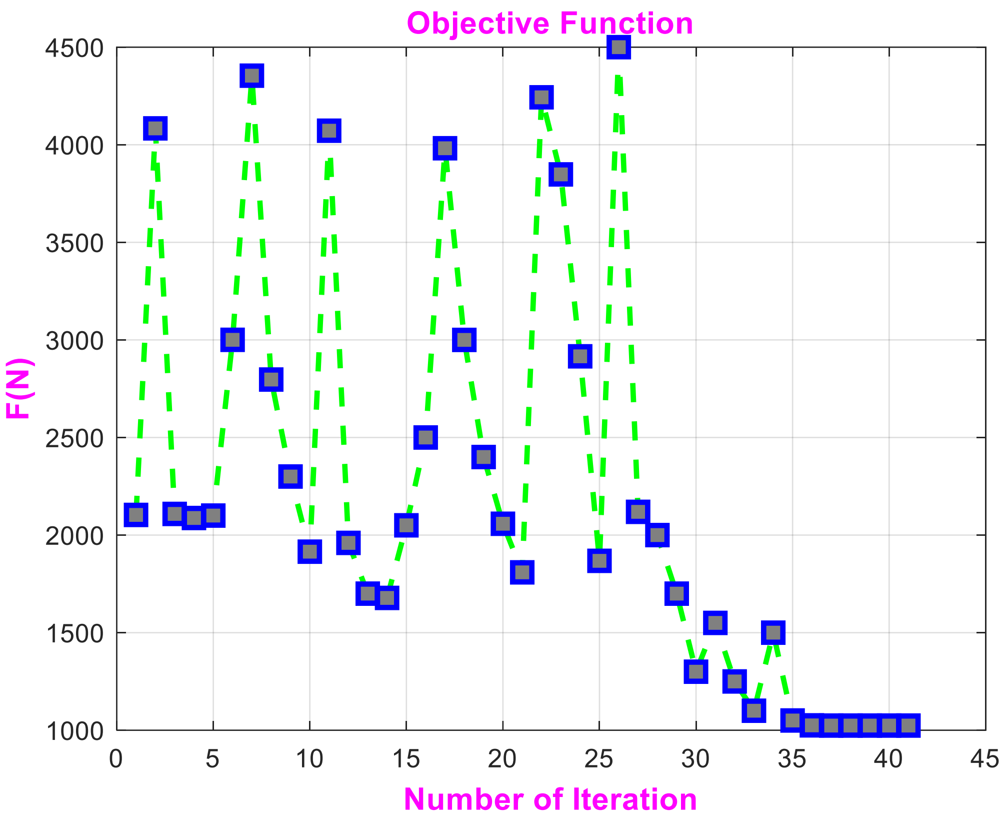

Figure.III.3 : Variation of the F(N) function

As the objective function is the cogging torque, which should be minimized, consequently the cost function should be minimized i.e. the set of the optimized variables for which the cost function is minimal represents the best solution of the optimization problem. Some of the optimization results, including the best set of the optimization variables for minimizing the cogging torque, are presented in Table.(III.1)

$$F\_1 = (G1 - 1)^2 * W1 \tag{III.1}$$

$$\text{where } G1 = 1+(\max(\text{abs}(Torque)) - 0.01) * 9 / 0.25 \tag{III.2}$$

$$F\_2 = (G2 - 8.55)^2 * W2 \tag{III.3}$$

$$\text{where } G2 = 1 + (Brad\_Avg - 0.5) * 9 / 0.31 \tag{III.4}$$

$$F(N) = F\_1 + F\_2 \tag{III.5}$$

Table III.1 : Variation of cost function through iterations

Evaluation	Hs0	PoleEmbrace	F(N)
1	4.63597521897031mm	0.663481551561022	1024.5
2	3.20944853053377mm	0.665398113956114	2119.7
3	3.9755851924192mm	0.829343546861171	4005.1
4	4.83556627094333mm	0.61324808496353	1868.5
5	2.00668355357524mm	0.746504104739525	2916.9
6	2.14831995605335mm	0.762422559282205	3848.1
7	3.26584673604541mm	0.881798760948515	4243.3
8	3.81188390758995mm	0.580349131748405	1809
9	3.24314096499527mm	0.636222418897061	2058.1
10	3.86938077944273mm	0.823361919003876	3982.1
11	2.01455732902005mm	0.542103335673086	1678.5
12	3.18326364940336mm	0.610745567186499	1960.1
13	2.95034638508255mm	0.829697561571093	4072
14	4.56053346354564mm	0.624613177892392	1915.6
15	2.5930051576281mm	0.72587359233375	2797
16	3.40720847193823mm	0.898046815393536	4354
17	3.29972228156377mm	0.647392193365276	2087.4
18	3.2563249610889mm	0.65394756920072	2108.4
19	3.74129459517197mm	0.851097140415662	4083.9
20	3.01223792229988mm	0.657353434858241	2103.3

In Table.III.1, the results are presented sorted per value of the cost function; the minimal cost function is on the top of the table. Figure.III.4 presents the two different rotor configurations of the basic (BM) and the optimized motor(OM) after the optimized variables hs0,and PoleEmbrace had been implemented in the design of the optimized model .Here it must be noted the machine configuration in Figure.III.4 (b)

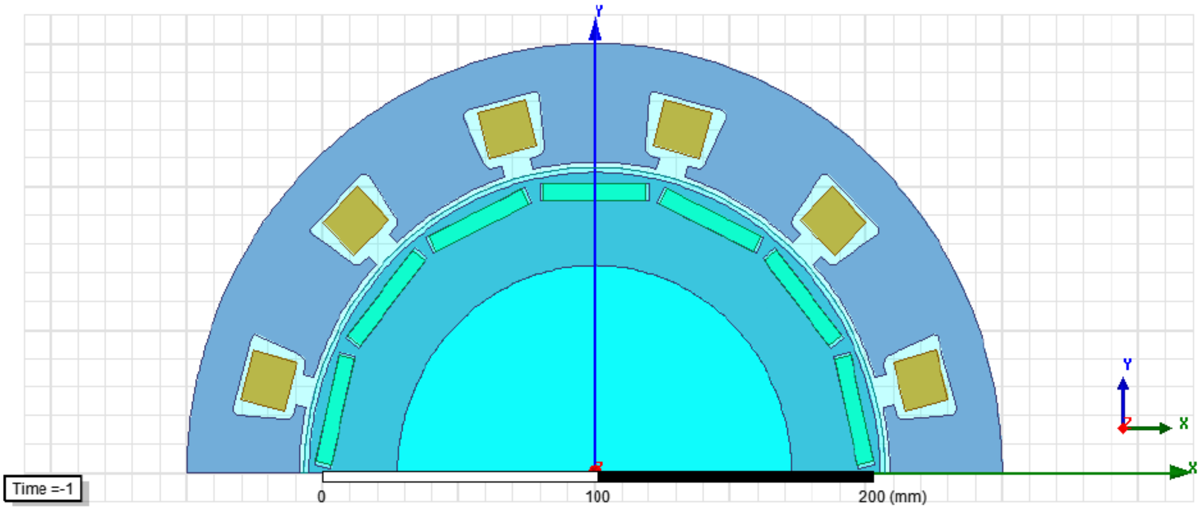

(a)Basic Motor

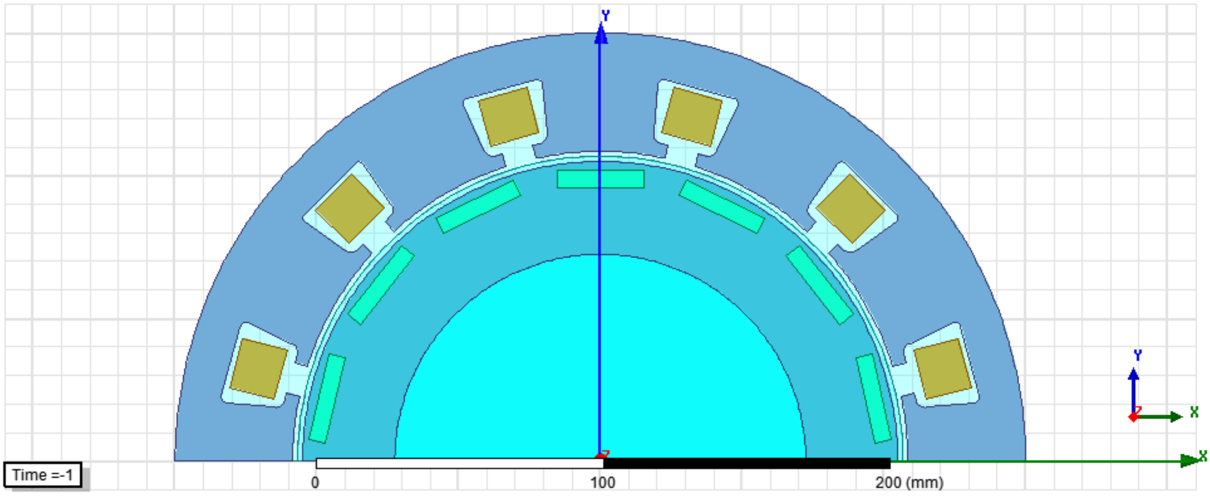

(b) Optimised Motor

Figure.III.4 : Machine configuration

III.5.1 Cogging Torque analysis

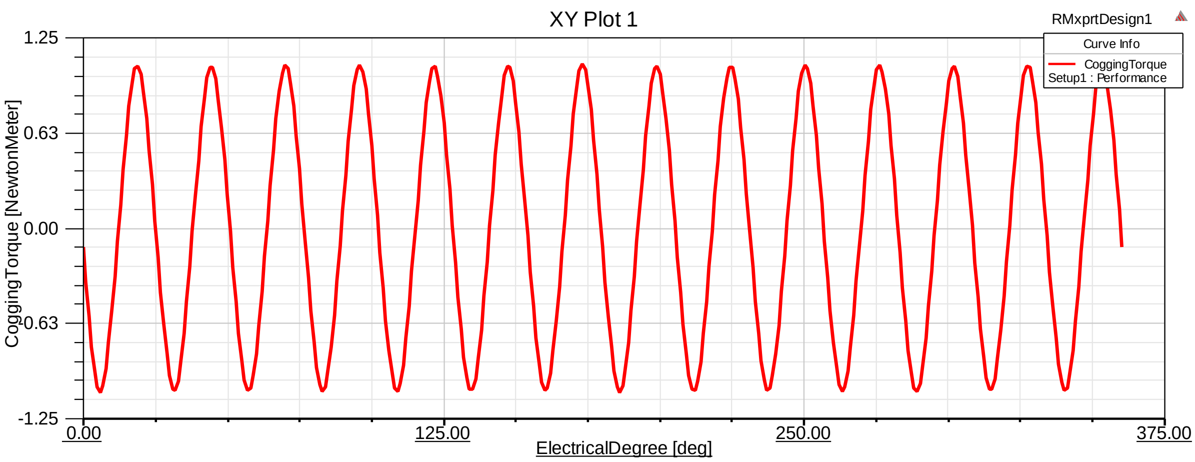

Figure. III.5 : Cogging Torque before optimisation

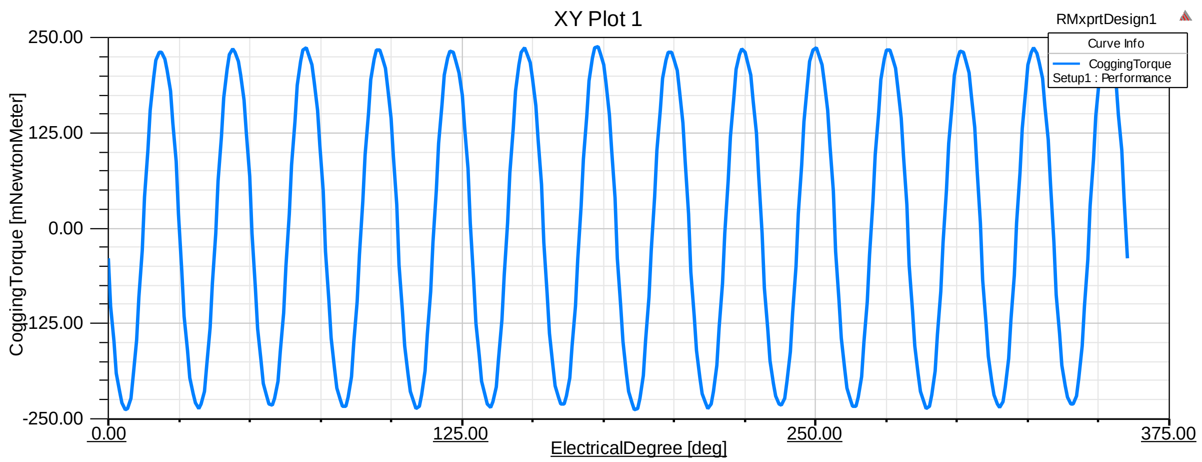

Figure.III.6 : Cogging Torque after optimisation

With the obtained set of the optimized variables hs0=2 mm, PoleEmbrace = 0.85, the new optimized model of the motor (OM) had been recalculated not only for the value of the torque are obtained when in the BM are replaced the best set of optimized variables.

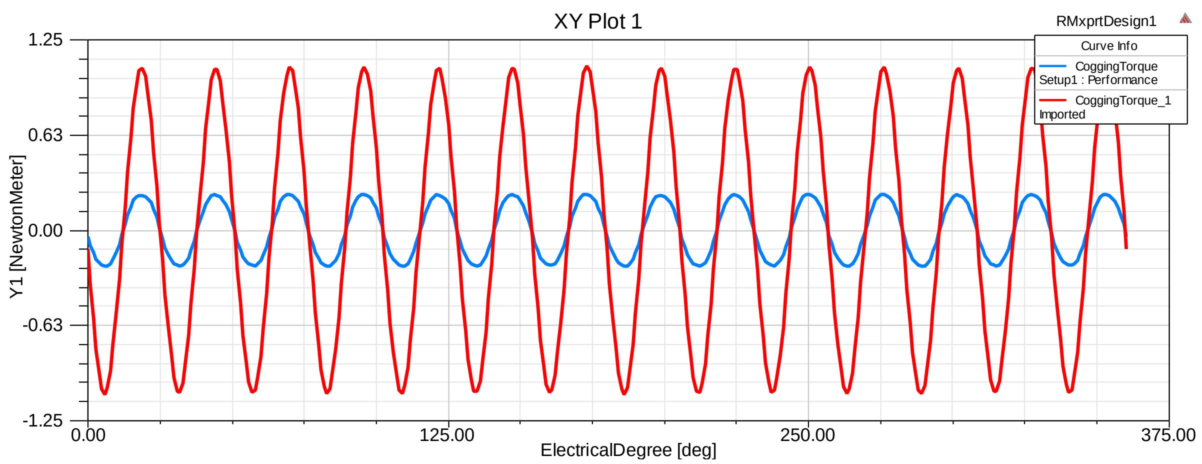

Optimised Desing: PoleEmbrace=0.9,Hs0=4mm

Nominal Desing: PoleEmbrace=0.85,Hs0=2mm

Figure.III.7 : Cogging Torque as a function of Electrical degree

III.5.2 Air-Gap Flux Density

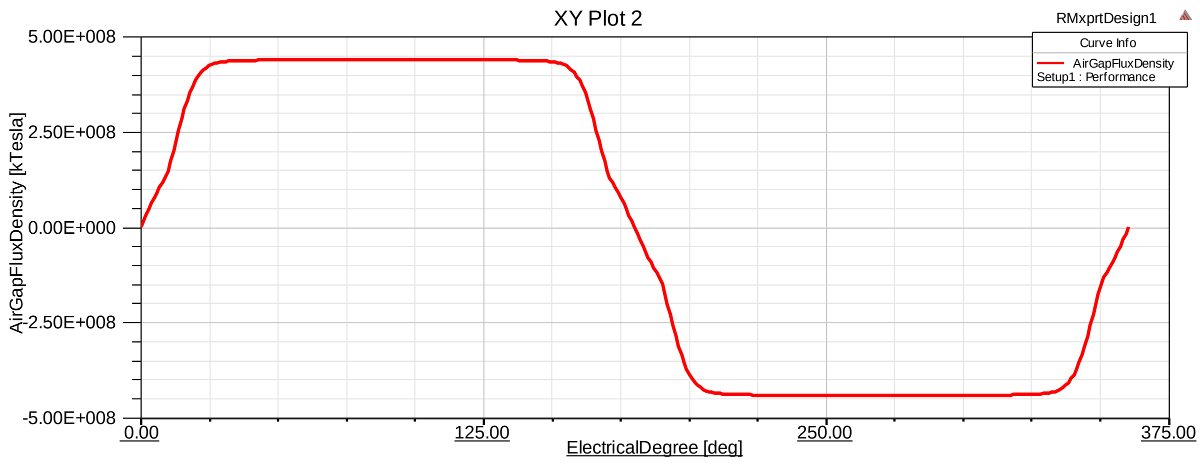

Figure.III.8 : Air-Gap befor optimisation

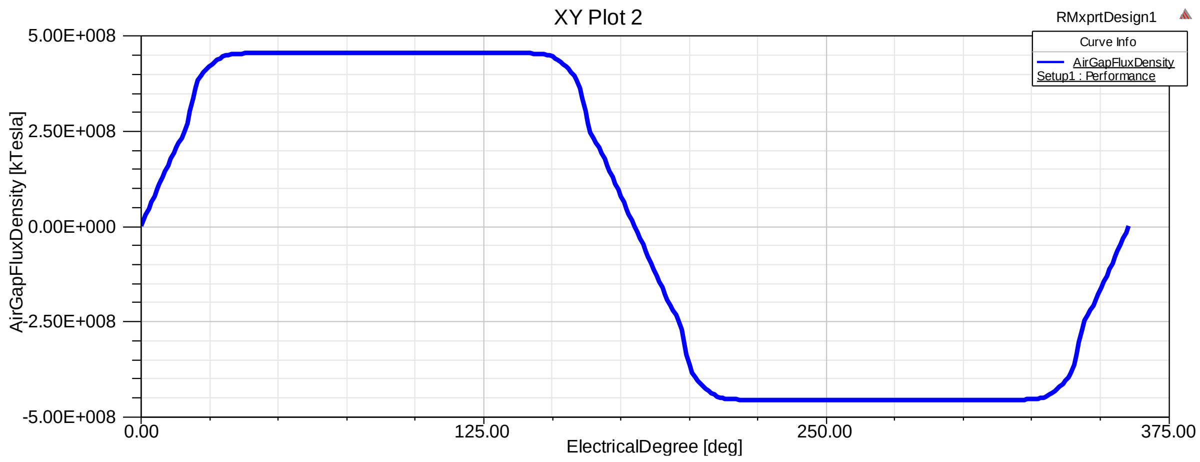

Figure.III.9 : Air-Gap after optimisation

The similar conclusions can be drawn by comparing the presented results of air gap flux density in Figure.III.10.

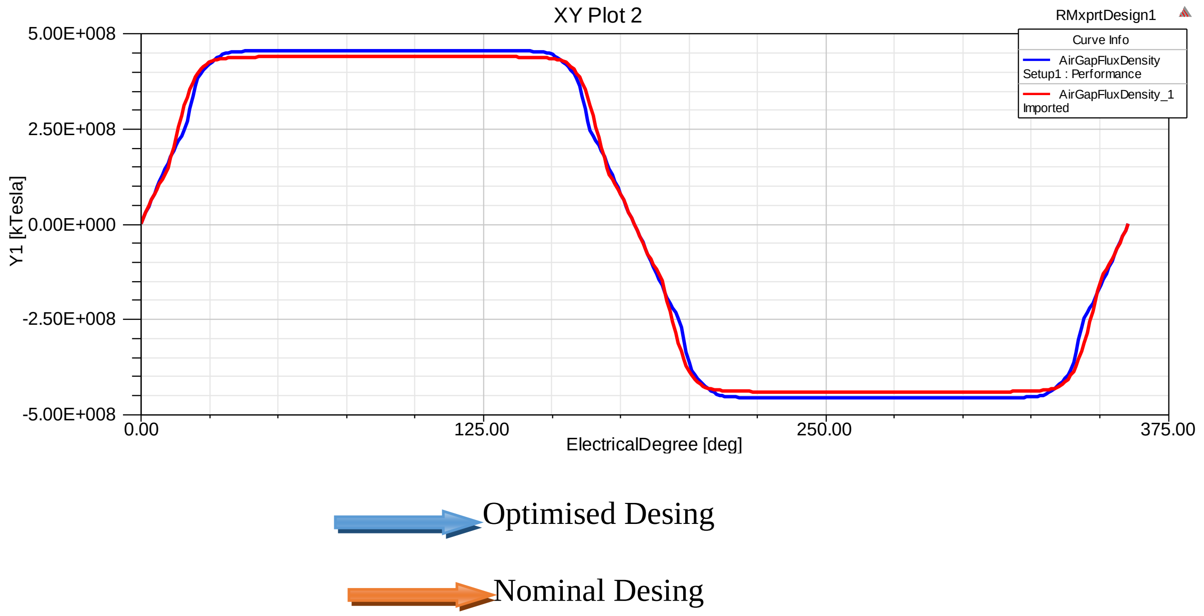

Figure.III.10 : Air-Gap Flux Density as a Function of Electrical degree

III.6 Plot B Field

Similarly Plot B field

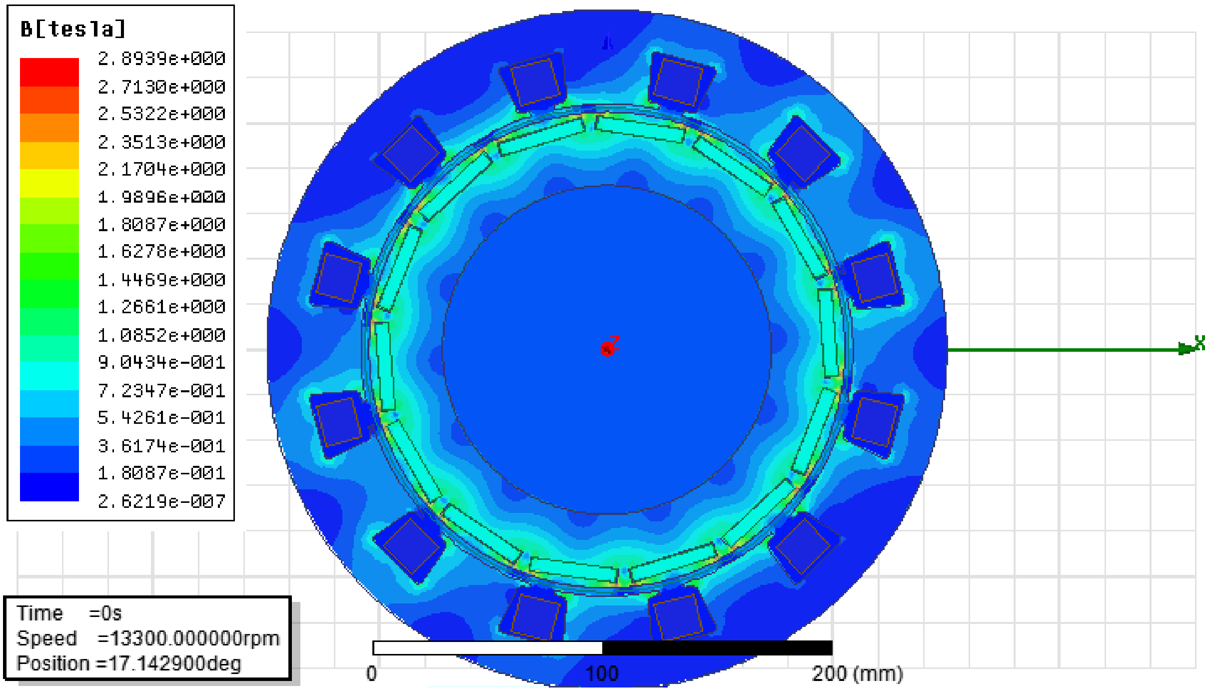

(a)-Basic Motor

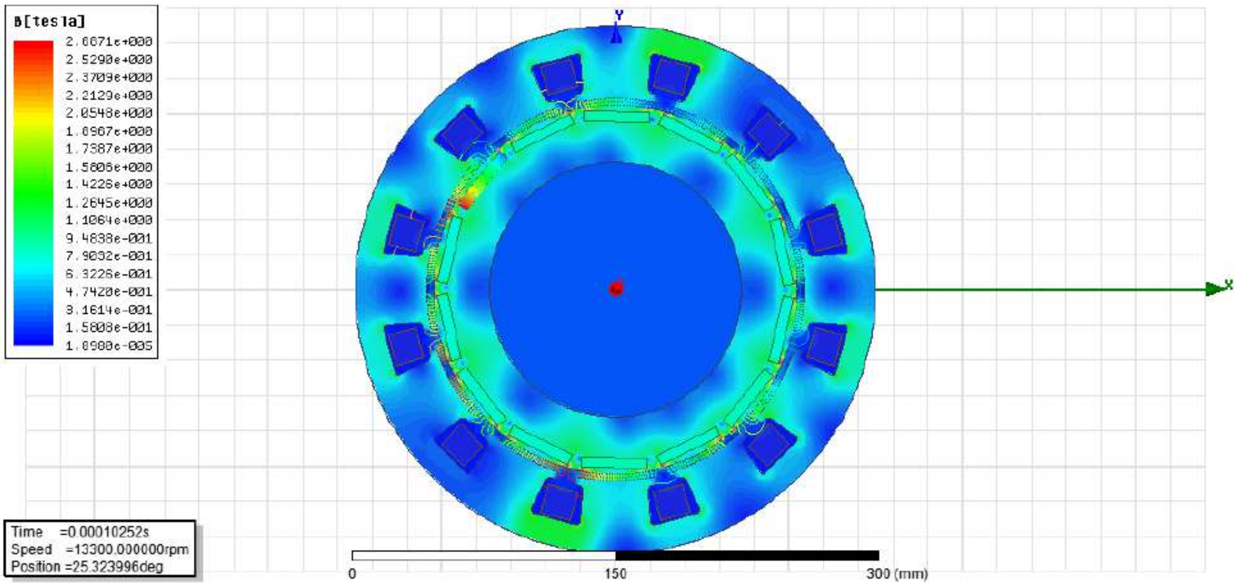

(b)-Optimised Motor

Figure.III.11 : Induction magnetique distribution in motor air gap

III.7 Plot Flux Lines

Similarly Plot Flux Lines

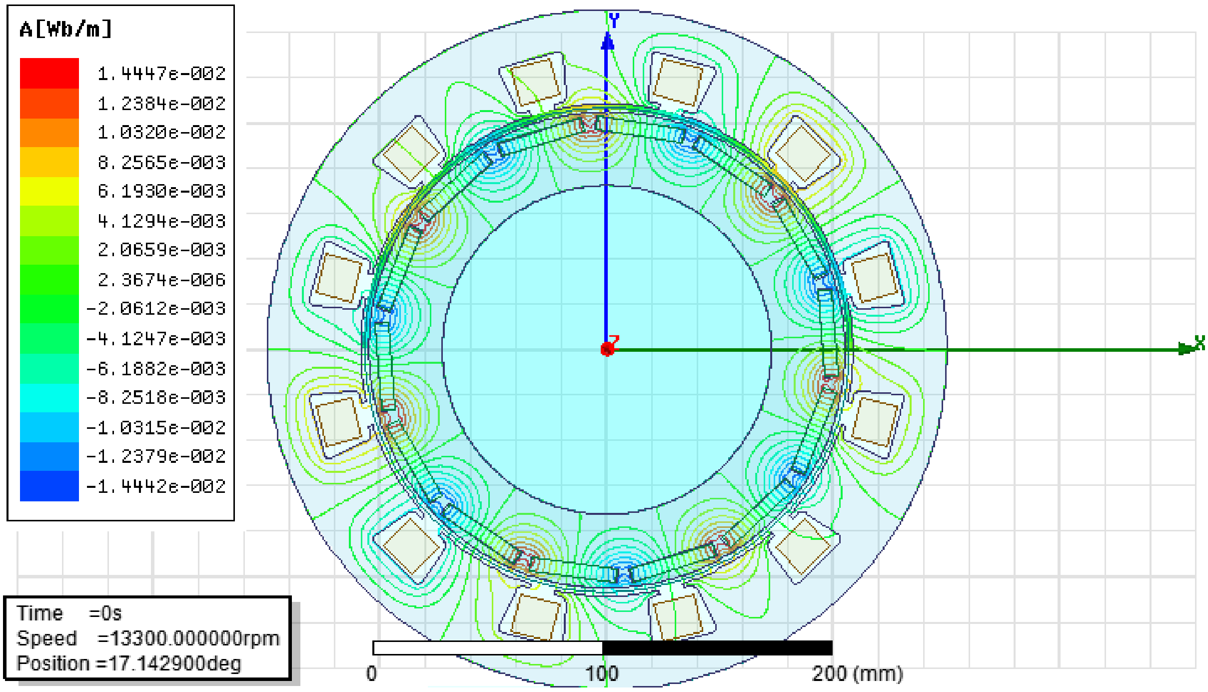

(a)-Basic Motor

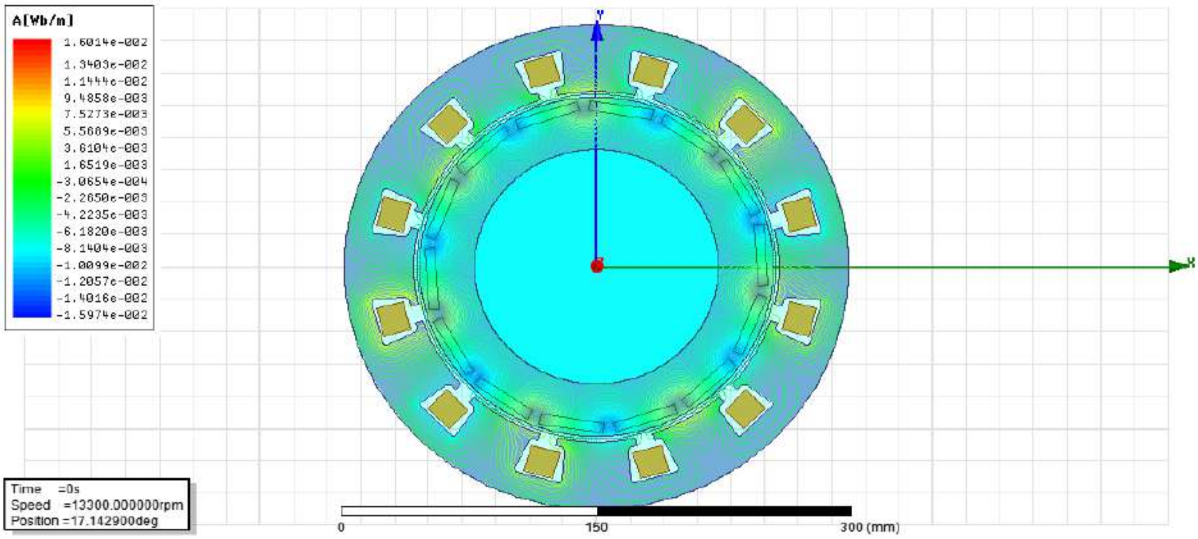

(b)-Optimised Motor

Figure.III.12 : Flux density distribution in motor air gap

III.8 Conclusion

In this chapter GA has been applied to this method to further reduce the simulation time. The GA simulation results indicate that the optimal design reduces torque pulsation . Radial forces acting on the stator teeth are also reduced in the optimal design, there by causing a reduction of the total deformation and the equivalent stress according to the structural analysis.This optimal rotor design is easily applicable in the manufacturing process compared to other rotor shape optimization methods.

General conclusion

General conclusion

In this end-of-study dissertation we studied the Synchronous Magnet Machine Permanent

In the first chapter we saw generalities on this machine like its constitution and its principle of operation as a generator and as a motor and we have seen also in this chapter the advantages and disadvantage of this machine. We have presented the different steps of maxwell exploitation. The latter can be used to solve partial differential equations . The present work shows the numerical model of software to compute the many parameters of machine.

In the second chapter This work is devoted to the study the effect of torque on Synchronous electric machines with permanent magnets Required. The finite element method was chosen because it is the simplest method Development with Maxwell program allowed us to determine the results of the magnetic flux and the Cogging torque.

Finally in the last chapter, the method of genetic algorithms is ap-plied in the optimization the minimization of the cogging torque in the synchronous permanent magnet motor magnets.optimization variables were included in the optimization problem.

From this study we can come out with a conclusion that says that the synchronous machine are very useful and too necessary machines for the human being.

Bibliographic references

.[1] Commande non linéaire de la machine synchrone à aimants permanents en vue du diagnostic des défauts

[2] SOURI, R., & BOUNACEUR, M. A. Simulation numérique des phénomènes Magnétodynamique de La Machine Synchrone à Aimants Permanents.

.[3] Liang, X., Wang, D., & Wang, M. Construction of Permanent Magnet Synchronous Motor Variable-Parameter Model

[4]Simulation numérique par élément finis d'une machine à aiment permanant (2020/2021 univ KASDI MERBAH OUARGLA)

. [5] Sakunthala, S., Kiranmayi, R., & Mandadi, P. N. (2017, August). A study on industrial motor drives: Comparison and applications of PMSM and BLDC motor drives. In 2017 International Conference on Energy, Communication, Data Analytics and Soft Computing (ICECDS) (pp. 537-540). IEEE.

[6] Tikhonova, O., Malygin, I., & Plastun, A. (2017, May). Electromagnetic calculation for induction motors of various designs by "ANSYS maxwell. In *2017 International Conference on Industrial Engineering, Applications and Manufacturing (ICIEAM)* (pp. 1-5). IEEE

[7]McDonagh, J., Palumbo, N., Cherukunnath, N., Dimov, N., & Yousif, N. (2022). Modelling a permanent magnet synchronous motor in FEniCSx for parallel high-performance simulations. *Finite Elements in Analysis and Design*, *204*, 103755.

[8] Cornejo, A. G. (2011). Maxwell-Faraday equation extension to four-dimensions. *Lat. Am. J. Phys. Educ. Vol*, *5*(4), 717

. [9] Pijush. K. Kundu, Ira. M. Cohen, "Fluid mechanics", Elsevier Science(USA), 2nd Edition 2002

[10]John J. Bloomer, Marcel Dekker, " Practical Fluid Mechanics for Engineering Application" Inc. New York, 2000

:[11] Zubayer, H. M. (2011). *Design analysis of line-start interior permanent magnet synchronous motor* (Doctoral dissertation, Memorial University of Newfoundland).

[12] Dusane, P. (2016). *Simulace BLDC motoru v ANSOFT Maxwell 3D* (Master's thesis, České vysoké učení technické v Praze. Vypočetní a informační centrum.).

[13]. Speed Control Of Permanent Magnet Synchronous Motor Using Power Reaching Law Based Sliding Mode Controller NavaneethanS1, Jovitha Jerome2 1assistant Professor, 2professor & Head Department Of Instrumentation And Control Systems Engineering PsgCollege Of Technology, Coimbatore, Tamil Nadu, India

[14].HAOUED MOUISSA, A., & HAMMOUDI, B. *2D simulation and study of the rotational magnetic separator* (Doctoral dissertation, UNIVERSITE KASDI MERBAH OUARGLA).

[15]Ayad A N I " Etude et Réalisation d'un séparateur à induction électromagnétique" thesis of PhD university of SIDI-BEL-ABBES May 2017

[16]L. A. O. V. D. Brauer, J. R..; Larkin, Finite Element Modeling of Permanent Magnet Devices. AIP -Journal of Applied Physics, 1984

[17] Ilka, R., Alinejad-Beromi, Y., & Yaghobi, H. (2018). Cogging torque reduction of permanent magnet synchronous motor using multi-objective optimization. *Mathematics and Computers in Simulation*, *153*, 83-95.

[18] Mishra, A. K., Rajpurohit, B. S., & Kumar, R. (2021). Revampment of surface permanent magnet synchronous motor design for ameliorated torque profile in e-mobility applications. *IET Electrical Systems in Transportation*, *11*(2), 99-108.

[19]Sarac, V. (2019). Performance optimization of permanent magnet synchronous motor by cogging torque reduction. *Journal of Electrical Engineering*, *70*(3), 218-226

[20] Aldoumani, M., Yuce, B., & Zhu, D. (2021). Using the Variable Geometry in a Planar Inductor for an Optimised Performance. Electronics, 10(6), 721.

[21]Kumar, M., Husain, D. M., Upreti, N., & Gupta, D. (2010). Genetic algorithm: Review and application. *Available at SSRN 3529843*.

[22]Soyaslan, M., Avsar, Y., Fenercioglu, A., & Eldogan, O. (2019, October). Cogging Torque Reduction in External Rotor PM Synchronous Motors by Optimum Pole Embrace. In *2019 3rd International Symposium on Multidisciplinary Studies and Innovative Technologies (ISMSIT)* (pp. 1-4). IEEE.